**Interactions between DNA and starch nanoparticles: adsorption and covalent attachment**

by

Alexander Chi Fai Ip

A thesis

presented to the University of Waterloo

in fulfillment of the

thesis requirement for the degree of

Master of Science

in

Chemistry

Waterloo, Ontario, Canada, 2013

## AUTHOR'S DECLARATION

I hereby declare that I am the sole author of this thesis. This is a true copy of the thesis, including any required final revisions, as accepted by my examiners.

I understand that my thesis may be made electronically available to the public.

Alexander Chi Fai Ip

## ABSTRACT

Biopolymers have been recently received more and more attention as a renewable substitute for traditional petroleum-based materials. Products made from petroleum-based materials typically cannot be recovered, with long term ramifications in sustainability and environmental concerns. Biopolymers such as starch are renewable, environmentally-friendly alternatives which have found additional use beyond their traditional roles as food substances as a biopolymer material, replacing their petroleum-based counterparts with comparable physical properties but also featuring long-term sustainable use. One such use is for starch to replace latex as a paper binder. Starch nanoparticles have seen tremendous development in use as a paper binder in place of traditional petroleum-based latexes, and other possibilities for the use of these starch nanoparticles are also being explored.

Nucleic acids have long been used by Nature as a carrier of genetic information. Recent advances in technology have allowed the fine manipulation of nucleic acids to take advantage of their inherent stability for roles beyond genetics. This includes the use of nucleic acids for bio-based sensing and for immunochemistry, which takes advantage of the chemical structure of nucleic acids for practical use.

In this thesis, the interactions between starch and deoxyribonucleic acid (DNA) biopolymers are investigated. The two biopolymers are found to adsorb to each other when dispersed in aqueous solution together. This can lead to the co-precipitation of the two biopolymers together out of solution in organic solvents such as ethanol. The generalizability of this interaction is explored, including its dependence on starch crosslinking, on the length and sequence of DNA, and the pH and salt concentration of the solvent. Fluorescence spectroscopy was used to characterize their interaction, supported by other similar techniques.

The covalent linkage of DNA and starch is also investigated. To this end, the appropriateness of using a starch-based nanoparticle with DNA coupling for drug delivery is considered. Starch is oxidized and covalently linked with DNA used as a targeting ligand and introduced to the HeLa cancer cell line. Various fluorescence-based techniques were used to monitor this interaction.

**ACKNOWLEDGEMENTS**

First and foremost, I would like to thank my supervisor, Dr. Juewen Liu, who has given tremendous support in guiding me along the course of my research. His kindness and openness is an inspiration for those in the academic field, and he has instilled in me and many others the passion for research. I would also like to thank my committee members, Dr. Shirley Tang and Dr. Vivek Maheshwari, for their valuable insight and insight in aiding my research. In addition, I would like to thank Dr. Michael Palmer, Dr. John Honek, and Dr. Gary Dmitrienko for the use of their lab space and equipment to complete work needed to be done.

I would like thank my many colleagues who have worked together with me in laboratory: Po-Jung Jimmy Huang, for his patience and forthrightness with training me in all the necessary techniques for my work; Dr. Neeshma Dave, for her kindness and eagerness to help with every aspect of tasks that need to be done; Dr. Xu Zhang, for his valuable input in ensuring the integrity of my data; Dr. Feng Wang and Biwu Liu, for all their assistance with equipment and discussions for ideas. It was definitely loads of fun working with you guys! The various undergraduate students I have worked with that have graced our laboratory with their input: James Maclean, Youssef Helwa, Thomas Kennedy, Kiyoshi Morishita, Rachel Pautler, Anand Lopez, and Janelle Tam; you have been a pleasure to work with, and the teaching goes both ways.

I would like to thank EcoSynthetix, Inc. and the many people standing behind them for the wonderful opportunity in this project. I would like to thank Nathan Jones, Ryan Wagner, Aareet Shermon and Abdel Rahman, the fourth-year nanotechnology engineering students who introduced me to this project with their fourth-year design projects; may your future endeavours be as successful as you are! To the Eco-WIN professors who have also offered many alternative angles to everything and expanded my learning that much more, I would like to thank Dr. Scott Taylor, Dr. Jean Duhamel, and Dr. Mario Gauthier; your tireless eagerness to discuss everything just how much progression we've made, and how much more still needs to be done. The same can be said of the other Eco-WIN graduate students: Duncan Li, Magda Karski, Ryan Amos, Joanne Fernandez, Wei Yi, and Lu Li; the many formal and informal gatherings we've had is a testament to the eagerness of everyone to share our inputs and knock our heads together. And of course a big thank you to Dr. Steven Bloembergen and Dr. Arthur Carty for assembling such a capable team to take on this challenge.

A big thank you to Dr. David Donkor, Eric Brefo-Mensah, Oscar Zhang, Shehan Salgado, and Anton van der Ven for helping with equipment I was not familiar with. You were all good company when I was working in your labs during those late hours. I certainly didn't want to be pressing the wrong buttons for those things! Further thanks go to Dr. Rob Donkers, Dr. Howard Siu, Laura Marrone, Dr. Eric Prouzet, Dr. Michael Tam, and Dr. Orion Bruckman for their continued guidance outside of classwork. It was always good to get additional perspectives outside of my immediate project, and to remind ourselves we all have lives beyond research.

My sincerest gratitude for my family, who have continued to support me throughout my tumultuous years through life. My mom and dad, Conita and Carson Ip, have never given up on me through my ups and downs of everything. My brother, Frederick Ip, who has endlessly inspired me to do everything; all my successes can be traced back to you. To my two friends who might as well be family, Angela Mui and Clara Wong, you've had to endure endless complaining and bickering from me, thank you for having the patience with me and sticking with me all this time.

Finally, to save the best for last, I would like to thank Imran Khimji, fellow classmate, lab member, and Eco-WIN collaborator, for all the discussions about anything and everything, in life, academics, athletics, and beyond, to all the pizzas and chicken dinners you made me have. I certainly owe a fair amount of my success to you, and if it wasn't for your support, I wouldn't have quite gotten as far as I have now. Unfortunately life takes us on different paths now, but I wish you all the best for everything you do, as you always have.

## DEDICATION

*To my parents, Carson and Conita Ip, who have never given up on me and supported me for everything I've done.*

## TABLE OF CONTENTS

## LIST OF FIGURES

Page

## LIST OF TABLES

Page

## LIST OF ABBREVIATIONS

DMSO: dimethyl sulfoxide

DNA: deoxyribonucleic acid

dsDNA: double-stranded deoxyribonucleic acid

EDC: 1-ethyl-3-(3-dimethylaminopropyl)carbodiimide

ENP: EcoSynthetix nanoparticle

EPR: enhanced permeation and retention

EDTA: ethylenediaminetetraacetic acid

FAM: 6-carboxyfluorescein

HEPES: 4-(2-hydroxyethyl)-1-piperazineethanesulfonic acid

MES: 2-(N-morpholino)ethanesulfonic acid

$MgCl_2$: magnesium chloride

mRNA: messenger ribonucleic acid

NaBr: sodium bromide

NaCl: sodium chloride

NaOH: sodium hydroxide

NCC: nanocrystalline cellulose

NEMO: nuclear factor-κB essential modulator

NHS: N-hydroxysuccinimide

PAGE: polyacrylamide gel electrophoresis

PCR: polymerase chain reaction

PEG: poly(ethylene glycol)

PLGA: poly(lactic-co-glycolic acid)

SELEX: systemic evolution of ligands by exponential enrichment

ssDNA: single-stranded deoxyribonucleic acid

TBE: tris-borate-EDTA buffer

TEMED: tetramethylethylenediamine

TEMPO: 2,2,6,6-tetramethylpiperidine-1-oxyl

## 1.0 INTRODUCTION

Petroleum-based products have long dominated the materials sector as inexpensive and easy-to-process materials. Building blocks made from petroleum-based polymer plastics are durable, easily processed, and possess excellent mechanical, thermal, and electrical properties. These non-biodegradable resources are immensely popular, with 26.7 million tons used in the USA annually.[1] Of those plastics, 11 million tons are then cast off as waste, mostly unrecoverable as they are typically a mix of many different types of polymers. The addiction of our society to these non-renewable resources will eventually lead to scarcity and associated rising costs for materials, as well as competing need for petroleum used for energy production.

It is of obvious importance that alternative materials are found to reduce our dependence on these non-renewable resources. Many biopolymers have been explored to see if they can match the cost, ease of processing, and physical properties of petroleum-based polymers, while retaining environmental friendliness and long-term sustainability.[2] Of these, starch has attracted considerable attention due to its already widespread use as a food substance, as well as its relatively low cost and well-established renewability. In addition, starch has already seen use in industrial non-food applications, including adhesives, cosmetics, surfactants, absorbents, binders, biodegradable fillers, coatings, and more.[3] These starches are harvested from foods already commonly grown as agricultural crops, such as potatoes, cassava, maize, or rice.

EcoSynthetix, Inc. has been working on replacing styrene-butadiene latex for paper binding using a starch-based derivative, in the process reducing the large starch granules into the nanoscale to allow smoother surface covering. Using a starch-based paper binder to replace the styrene-butadiene would replace a non-renewable resource with a renewable one, adding to the sustainability aspect of large-scale paper manufacturing. The success of their product in this field has allowed EcoSynthetix to consider other applications of their product, where substitution of petroleum-based products by renewable biopolymers can be further realized.

Deoxyribonucleic acids (DNA) have been historically known to be a carrier of genetic information. Nature has selected this particular class of biopolymers for this purpose due to their high thermal stability and resistance to degradation, making them ideal carriers for long-term storage of genetic coding. While small changes can occur due to mutation, it does not require constant duplication like proteins or other biopolymers may require.

Recent advances in chemical synthesis techniques have allowed the manipulation and synthesis of DNA strands independent of biological processes. Custom-designed DNA strands can be made with virtually any sequence we desire, and cheaply duplicated in bulk. This has allowed us to take advantage of the high stability of these DNA strands for purposes beyond cellular functions. These functions include bio-based sensing and immunochemistry, and have many tangible benefits over existing methods of using antibody-based methods.[4] This has allowed us to diversify the use of nucleic acids for functions other than being a carrier for genetic information.

## 1.1 Research Objectives

The objective of this research is to characterize a starch-based nanoparticle formulation produced by EcoSynthetix, Inc., which has been their flagship product and has led to its commercial success. EcoSynthetix, Inc. has expressed a desire to expand the use of their product to other niches, but would need to further determine its capabilities before doing so. In addition, its material properties can be improved by the functionalization of these starch nanoparticles with various ligands. One potential use of this would be the attachment of DNA ligands onto starch nanoparticles, and use the starch nanoparticles as a drug delivery vehicle for the treatment of cancer.

Over the course of the research, it has also been found that the starch nanoparticles can be used to assist in the precipitation of DNA out of solution with high efficiency. This method has been found to be much simpler and faster than traditional DNA precipitation techniques, with comparable results. In addition, the materials required are much more easily obtained and, in line with the goal of sustainability, do not require petroleum-based products to precipitate out DNA. As an additional goal of the research was to elucidate the conditions for which this DNA precipitation can occur through non-covalent adsorption onto the starch nanoparticles.

Finally, the covalent attachment of DNA onto starch was explored. A specific strand of DNA was used, which was known to have high targeting efficiency to cancer cells, to see if it can induce endocytosis by the cell. If the starch nanoparticle was then loaded with antineoplastic drugs, it could aid in the site-specific delivery of these antineoplastic drugs as part of cancer therapy.

## 1.2 Thesis Outline

This thesis will cover the interactions of starch and deoxyribonucleic acids, both through physical adsorption and covalent attachment, and explore potential applications to these effects. The thesis is organized into 5 chapters. Chapter 2 will give a more in-depth review of starch and DNA as materials, starting from its chemical makeup and progressing to secondary and/or tertiary structures that result from its interactions with itself, concluding with established applications using solely those materials as related to this thesis. Chapter 3 will address the physical adsorption of DNA onto starch nanoparticles. The physical adsorption of starch and DNA were characterized using fluorescence spectroscopy, and supplemented with gel electrophoresis. Chapter 4 will cover the covalent attachment of DNA onto starch nanoparticles. The covalent attachment of DNA onto starch was characterized using a host of techniques, including fluorescence spectroscopy, gel electrophoresis, and fluorescence microscopy. Chapter 5 summarizes the work performed in this thesis, and provides insight as to further directions that can be taken. As this thesis is part of a broader collaboration, it is expected that the data and conclusions presented here can be used to facilitate additional research with starch and DNA interactions and bring them to further practical application.

## 2.0 STARCH AND DNA

Starch and DNA are both naturally-occurring biopolymers easily found in nature. Both are well-characterized with a long history of research interest from their biological roles as energy storage and genetic information carrier, respectively. Recent advances in chemical understanding and biotechnology have allowed for these materials to be synthetically modified for purposes beyond their biological roles. These purposes utilize the physical and chemical properties of the biopolymers, and include using starch as a bio-latex for paper binding to replace petroleum-based plastics, and using DNA as aptamers to replace the highly variable antibodies for immunochemistry and bio-based sensing. Additional applications are pending from the rapid research interest being poured into these newly rediscovered materials.

### 2.1 Starch and Starch Nanoparticles

Starch is a carbohydrate biopolymer found abundantly in nature from many sources. It is used in plants as a method for high-density energy storage, built up from individual glucose units produced via photosynthesis. Many foods common in the human diet such as potatoes, wheat, maize, rice, oats, and cassava (tapioca) often contain high amounts of starch, and these sources are typically used for harvesting starch. As a food additive, starch has seen use as a binder, thickener, and glazing agent.[3] As an inexpensive renewable biopolymer, starch is also used, either in its native form or chemically modified, for industrial non-food purposes as a replacement to other traditional materials. Such uses include as adhesives, cosmetics, surfactants, biodegradable fillers, flocculants, and coatings.[3] Unfortunately, these plant starches are most commonly found in the form of granules; these relatively large particles, ranging from 1-100 μm, make thorough modifications at a chemical level difficult.[5] Understanding their chemical structure has allowed thorough modification of starch components and process them for bulk modifications. Different techniques can be used to reduce the size of starch particles to make its functional groups more accessible to chemical modifications. These modifications can improve properties such as hydrophilicity, viscosity, acid resistance, and add functional groups for further processing.[6]

### 2.1.1 Physical Properties

Starch is usually found as a white powder that is tasteless and odourless. It has poor solubility in cold water or ethanol, but while dispersed in water starch can gelatinize with the addition of heat above 70°C, allowing it to dissolve.[7] If returned to lower temperatures, starch can retrograde, becoming even less soluble in water and gaining enzymatic degradation resistance. Starch will also act as a shear thickener in water. In basic conditions above pH 9, starch may degrade, with a pronounced effect observed at pH 10 and above.[8]

#### 2.1.1.1 Primary Structure

The main constituent for starch is glucose. While in solution glucose is predominantly found in the cyclic pyranose form, and is also similarly formed while polymerized as starch. The glucose units in starched are linked together via α-1,4 glycosidic bonds in linear form, and via α-1,6 glycosidic bonds in branched form. The bonds are susceptible to hydrolysis, but rates vary depending on its secondary structure. In cellular respiration, glucose must first be hydrolyzed from starch before glycolysis can occur. Enzymes such as α-amylase, produced in the pancreas and also found in saliva, can be used to break down starch into simpler saccharides for digestion.

#### 2.1.1.2 Secondary Structure

Starch has two major constituents that form its secondary structure.[5,9,10] The first is amylose, which consists of glucose linked together by almost exclusively α-1,4 glycosidic bonds, giving it a linear characteristic. The linearity allows for hydrogen bonding to occur between consecutive glucose units, giving rise to a helical structure that can be tightly packed. The tight packing renders the interior to be less accessible for reactions to occur. This structure also prohibits water from reaching the inner structure, giving amylose its insolubility in water. Amylose can have a molecular weight in the $10^5$-$10^6$ g/mol range,[11] consisting of thousands of glucose subunits. The other secondary structure for starch is amylopectin, which has α-1,6 glycosidic bonds present every 12-20 glucose units in addition to α-1,4 glycosidic bonds (Figure 2.1A-B).[9] This branching allows clusters of chains to gather at regular intervals. The openness from branching also allows water to penetrate, increasing its overall solubility. Compared to amylose, amylopectin is a much larger molecule, with molecular weights in the $10^6$-$10^7$ g/mol range.[11] Typical starch particles have a weight ratio of 20-30% amylose and 70-80% amylopectin, depending on the source of the starch.[9]

Glucose-based isomers to starch exist that proliferate in nature. The most common is cellulose, typically found in cell walls of plants and certain bacteria. Cellulose differs from starch such that they consist of β-1,4 glycosidic bonds; this allows for more compact stacking and lack of recognition from amylases. Dextran is another isomer; this polysaccharide features primarily α-1,6 glycosidic bonds, occupying the primary hydroxyl group on the 6′ carbon. This structural difference allows for different packing between chains of the polysaccharides (Figure 2.1C-D).

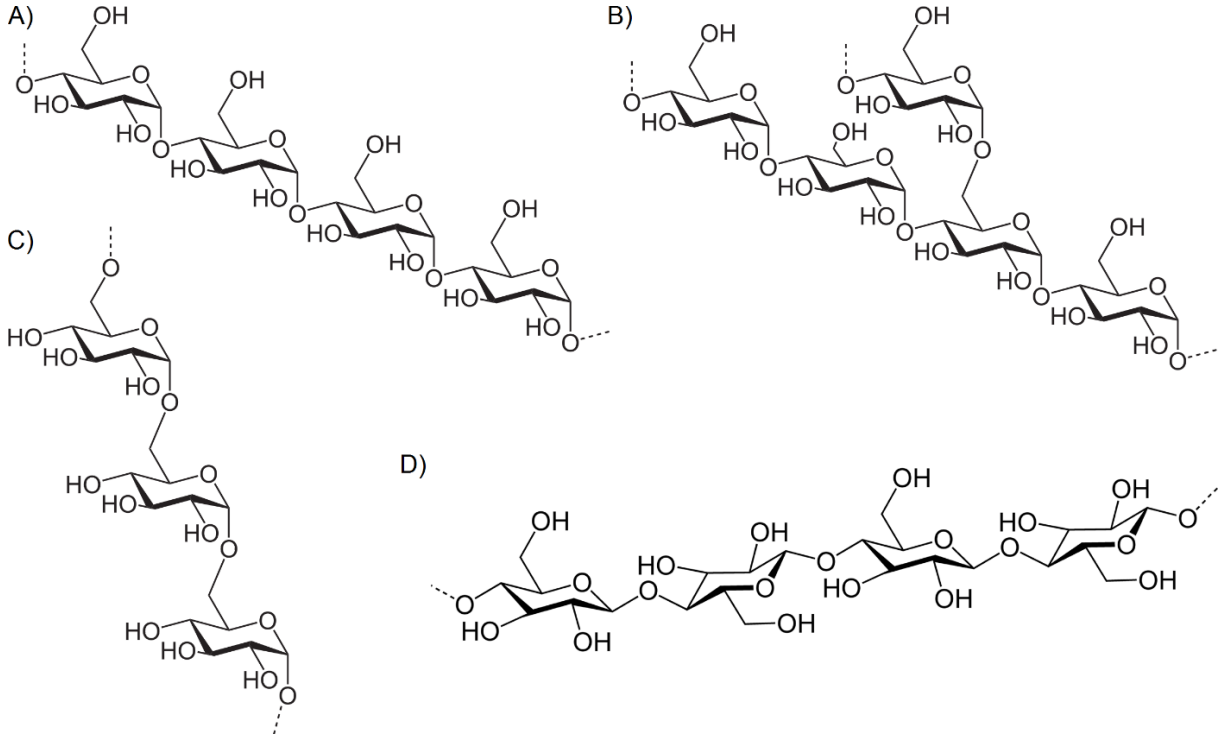


**Figure 2.1**: Molecular structures of glucose-based polysaccharides. A) Amylose with predominantly α-1,4 glycosidic bonds B) Amylopectin with both α-1,4 and α-1,6 glycosidic bonds C) Dextran with predominantly α-1,6 glycosidic bonds D) Cellulose with β-1,4 glycosidic bonds.

### 2.1.1.3 Tertiary Structure

Typically, starch is stored in plants as granules; these granules can vary widely in size depending on the species of the plant, from 1 μm found in taro roots to 100 μm found in potatoes.[9] Likewise, starch granule shapes can also vary according to their species origin (Table 2.1). The size and shape of the starch granules will affect the ease of bulk processing, although the chemical constituents of the granules remain largely the same.

**Table 2.1**: Size and shape of starch granules from various plants

| Plant Species | Granule shape | Granule size (μm) |
|---|---|---|
| Taro[12,13] | Polyhedral | 1-5 |
| Rice[5] | Polyhedral | 3-8 |
| Wheat[5] | Spherical, lenticular | 2-10, 15-35 |
| Oat[10] | Oval | 2-15 |
| Peas[5] | Rentiform (kidney-shaped) | 5-10 |
| Maize[5] | Spherical, polyhedral | 2-30 |
| Cassava (Tapioca)[5] | Spherical, lenticular | 5-45 |
| Potato[5] | Lenticular | 5-100 |

The internal structure of a granule is mostly determined by the larger amylopectin units, which dominate the arrangement found inside (Figure 2.2). The periodic branching found in amylopectin separates the region into crystalline and amorphous lamellae with a periodicity of 9 nm.[9,14] The crystalline lamellae are formed when clusters of adjacent linear side chains form double helices which pack together in a crystalline structure. Amorphous lamellae are formed with the remaining clusters of branching that occurs in amylopectin. These repeating lamellae form a semi-crystalline zone, which is also separated by another amorphous zone, which together form a "growth ring". This amorphous zone would contain both amylopectin and amylose, found in a disorganized state.[15] The growth rings are concentric and also have its own periodicity of several hundreds of nanometers,[9] and together form a starch granule.

The structure of a starch granule can be irreversibly disrupted by raising its temperature above 70°C; the exact temperature required for this disruption varies based on the size of the granule, but all granules undergo the same process when the temperature is raised sufficiently high. This disruption is termed gelatinization, and can be characterized by the loss of crystallinity in the starch granule, accompanied by a swelling of the granule through water absorption and leaching of amylose molecules out of the granule.[16] The gelatinization of the starch granules can be monitored by the loss of birefringence in the crystalline lamellae in the starch granules, and more accurately, by X-ray scattering. Typically, starch gelatinization begins with the absorption of water in the amorphous regions of the granule. As amylose is leached out from the amorphous regions, this allows for more water absorption. Crystallinity is lost only after crystalline regions are completely disrupted due to further temperature increase, as observed by X-ray scattering.

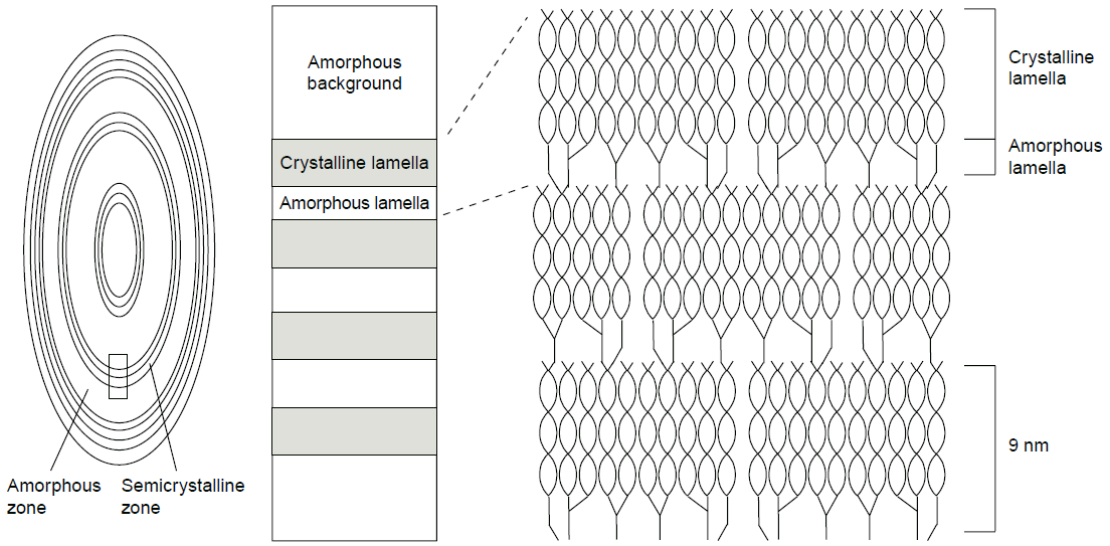


**Figure 2.2**: Amylopectin packing structure determining lamellar regions.[14] The growth rings with the amorphous and semicrystalline zones can be shown. The semicrystalline zone is further broken down to crystalline and amorphous lamella, which are driven by the double helical and branched portions of amylopectin, respectively. Reprinted with permission.

Starch that has undergone gelatinization may undergo retrogradation after temperature is reduced back to below gelatinization temperature. The crystallinity that was lost from gelatinization is slowly reformed from the amylose chains re-establishing a more thermodynamically stable double-helical structure.[3] Water is also expelled from the gel matrix during this reformation as syneresis.[17] This re-establishment typically proceeds with shorter amylose chains occurring first, followed by longer amylose chains.[18] Amylopectin chains, on the other hand, take even longer to retrograde, but reinforce the amylose structures in increasing crystallinity.[19,20] Fully retrograded starch typically has superior properties compared to the original starch granules in terms of crystallinity and rigidity, due to the combination of the crystalline and amorphous regions of the granule into an almost fully crystalline construct.[17] In addition, the solubility of retrograded starch in water becomes even lower than the native granules due to the inability for water to penetrate the crystalline structures. This retrograded starch also experiences resistance from digestive enzymes such as α-amylase both due to its higher packing and lower solubility in water, rendering its glycosidic bonds less accessible for the enzyme to hydrolyze.[3,21] Some starches can be coupled with lipids that disrupt crystalline structure; this makes the starch accessible for digestion by enzymes. However, the lipids also add to the insolubility of the starch from hydrophobicity, adding to the digestion resistance.[22]

### 2.1.2 Preparation of Internally Crosslinked Starch Nanoparticles

The incorporation of crosslinking agents into starch is one method to improve the material properties of starch. Crosslinking agents are used to chemically bind two or more polymer chains together, holding them in place relative to each other. Depending on the polymer, different macroscopic effects can be seen as a result of this, including a rise in rigidity, tensile strength, and shear strength. Many crosslinking agents have been explored to supplement the properties of natural starch. For a crosslinking agent to be viable, it must have at least two sites for which it can react with starch; the most commonly available would be the hydroxyl groups on the 2′, 3′, and 6′ carbons (Figure 2.3). Candidates for crosslinking agents include phosphorus oxychloride[3], sodium trimetaphosphate,[23] sodium tripolyphosphate,[24] epichlorohydrin,[25,26] 1,2,3,4-diepoxybutane,[27] glyoxal,[28] and citric acid.[29]

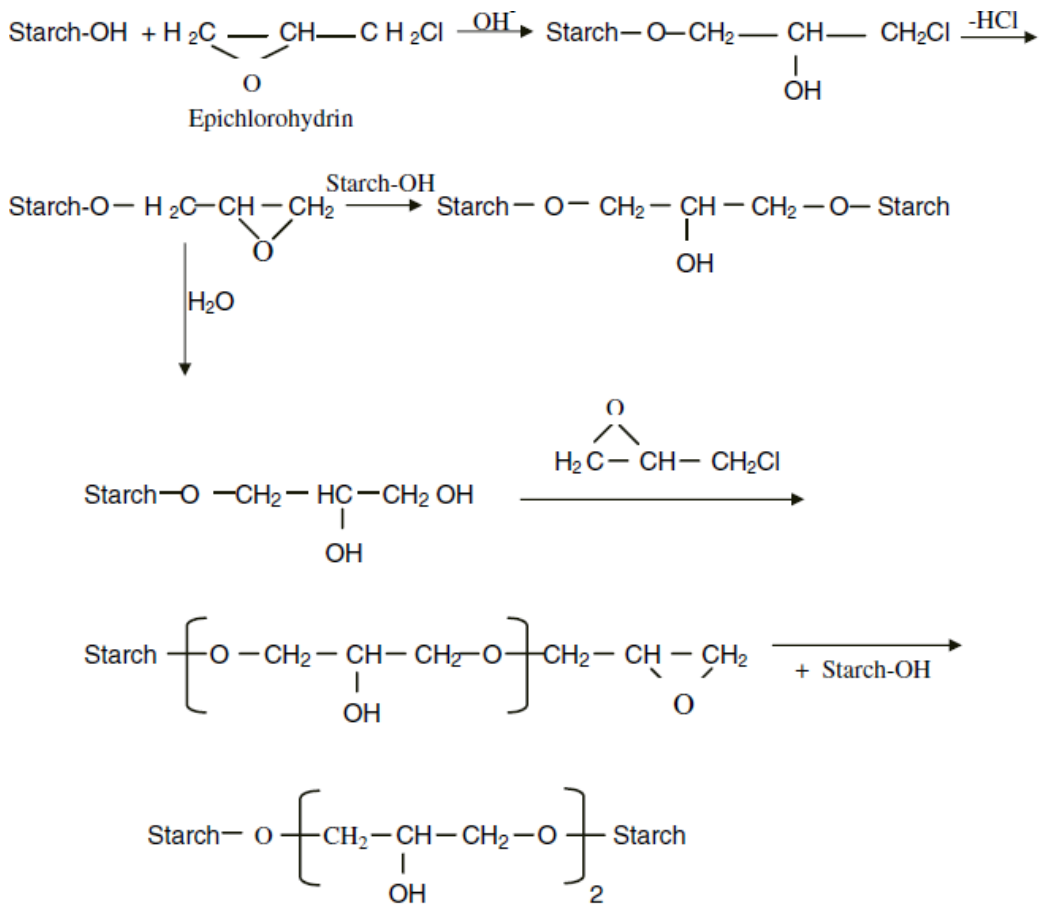


**Figure 2.3**: Crosslinking of starch using epichlorohydrin as crosslinking agent.[26] Reprinted with permission

These modifications typically improve the material properties of starch for various applications, including tensile strength, shear strength, and resistance to acid, temperature, and retrogradation. These crosslinking reactions typically require basic conditions,[6,23,25,27,30] which may be harmful to the starch backbone itself.[8] In addition, certain crosslinking agents have other safety considerations that would make them unsuitable for food use, such as the carcinogenic epichlorohydrin.[31–33]

### 2.1.3 Starch Nanoparticles Prepared by Reactive Extrusion

Reactive extrusion for the preparation of starch nanoparticles is a combination of several technologies that optimized conditions for additional modifications on the starch structures. Batch reaction of starch typically takes place in a continuously stirred tank reactor. As starch has low solubility in ambient conditions, dissolving it would require raising the temperature inside the tank to above 60°C. This would cause the starch granule structure to be disrupted and the starch will gelatinize, giving a more uniform mixture, but also becoming much more viscous and difficult to manage[34]. Instead, batch reactions are performed at under 60°C with only 35-45 wt% starch and mixed with 10-30 wt% sodium chloride or sodium sulfate to aid in dissolution. The comparatively low starch concentration, as well as the presence of salt that typically must be removed from the final product, leads to suboptimal reaction selectivity and comparatively long reaction times of 2-24 hours.[34]

The use of a reaction extruder (Figure 2.4) alleviates some of these issues, allowing for greater control of reaction parameters. By design it is well-suited for handling fluids of high viscosity,[34] as is the case of gelatinous starch, and provides excellent control of mixing, heat transfer, shear rate uniformity, and residence time.[35] The addition and removal of reagents and by-products is also better controlled with a reaction extruder. For starch, concentrations as high as 60-80 wt% can be used, with reaction temperatures in the 70-140°C range, and a residence time as low as 2-5 minutes is recommended. Up to 15-fold rate enhancements have been reported.[34] A side effect is that the shear rate as a function of mechanical energy input can drastically degrade starch, causing a sharp reduction in molecular weight.[34,35]

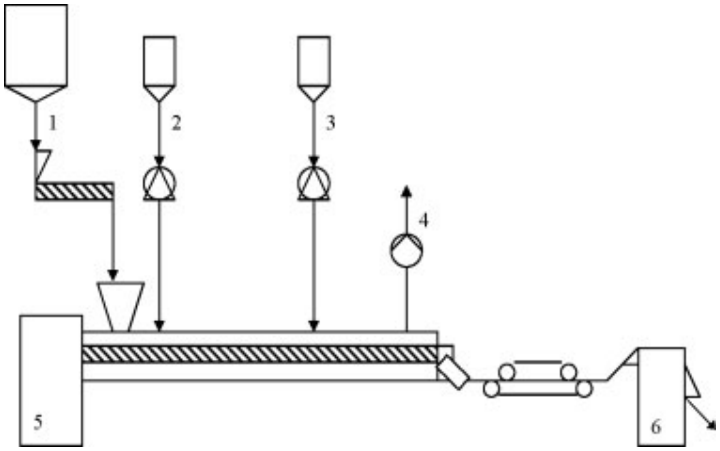


**Figure 2.4**: Typical setup of a reactive extrusion system for starch.[35] **1:** weight feeder for starch; **2,3**: metering pump; **4**: vacuum pump; **5**: twin-screw extruder; **6**: forced strand pelletizer with "dry" cut. Reprinted with permission.

### 2.1.4 Starch Nanoparticles for Drug Delivery

As starch is a natural polymer with well-documented properties, there has been much research interest devoted into using it as a carrier for drug delivery. Various modifications have been introduced in an attempt to make starch small but sturdy enough to be carried through the circulatory system while carrying therapeutics to a site of interest. These modifications include crosslinking to form a gel-like structure for encapsulating therapeutics, functionalization for addition of other ligands for targeting and/or stability, and many more.

Crosslinking agents used for material strengthening in industrial processes can also be used for controlled release of therapeutics. Theophylline for the treatment of asthma can be encapsulated in a crosslinked amylose delivery system using epichlorohydrin as the crosslinking agent to extend drug release times up to a period of 15 hours while maintaining a linear release profile.[36] Similarly, sodium tripolyphospate and sodium trimetaphosphate were used as crosslinking agents to create starch nanoparticles via an oil/water emulsion.[37,38] Alternatively, starch can be functionalized with additional groups such as propyl groups,[39] oleic acid grafts,[37] or aldehydes through oxidation,[40,41] for additional ease of synthesis and nanoparticle formation. For example, propyl-starch was utilized in a starch nanoparticle formulation to grant additional hydrophobicity. This additional hydrophobicity was used to allow manipulation using low-toxicity organic solvents such as ethyl acetate.[39] The nanoparticle itself was explored for use as a transdermal drug delivery device.

## 2.2 DNA

DNA is another biopolymer found in all living organisms as a carrier of genetic information. It consists of 4 major subunits, called nucleotides, which is able to code for the necessary amino acids in proteins. DNA is typically found as a double-stranded helix, with the nucleotides bound to each other through hydrogen bonding, and an alternating deoxyribose and phosphate backbone facing outwards. The nucleotides used are the purines adenine and guanine, which are paired with the pyrimidines thymine and cytosine respectively. This backbone is stable and resistant to degradation, allowing for the long-term storage of genetic information. In living organisms, DNA can be typically found in a single circular chromosome and surrounding plasmids in prokaryotes, and as part of linear chromosomes contained within a nucleus in eukaryotes.

Advances in technology have allowed the creation of synthetic DNA *ex vivo*. In particular, almost any arbitrary sequence of DNA can be constructed from individual building blocks through solid-phase synthesis,[42,43] allowing custom-made DNA oligomers for various interactions. In addition, polymerase chain reaction (PCR) has allowed the mass production of specific DNA sequences for additional characterization and application. This has lowered the production costs associated with DNA, and its newfound affordability has allowed DNA to be used for many purposes beyond its role as a genetic carrier, including use in bio-based sensing and in immunochemistry.

### 2.2.1 Physical Properties

The famous X-ray crystallography image of DNA taken by James Watson and Francis Crick illuminated the structure of DNA and became the basis for many other important discoveries of the macromolecule. It was then that the double helix structure of DNA was determined, with a pitch of 34 angstroms and a radius of 10 angstroms.[44] The strands are joined together in an anti-parallel fashion; these complementary strands run in opposite directions of each other as determined by the 5′ and 3′ ends denoted by the carbon number on the deoxyribose sugar. DNA sequences are traditionally listed from the 5′ end to the 3′ end. In neutral and basic conditions, DNA is found to be negatively charged, as the phosphate backbone becomes deprotonated and DNA as a result becomes polyanionic.

### 2.2.1.1 Primary Structure

A DNA macromolecule contains many nucleotide subunits which are joined together to create a long continuous polynucleotide chain. Each nucleotide consists of three parts: a phosphate and 2-deoxyribose sugar forming the backbone, and a nitrogenous base which is the primary genetic storage element (Figure 2.5). The four nucleobases, adenine, thymine, guanine and cytosine, form a quaternary system for amino acid coding, which can be converted into a polypeptide via ribosome translation. The nucleobase is bound to the 2-deoxyribose via the 1′ carbon, while the phosphate is bound to the 5′ carbon. Subsequent phosphates of additional nucleotides are bound to the 3′ carbon of 2-deoxyribose. The phosphates can become deprotonated in neutral and basic conditions, giving DNA a net negative charge.

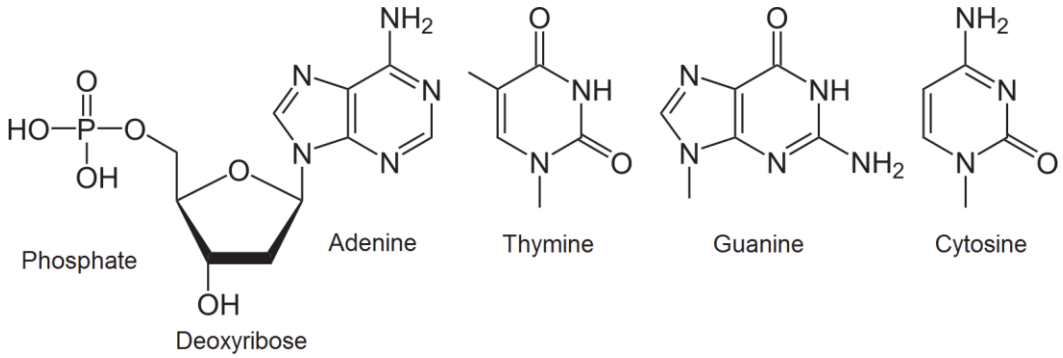


**Figure 2.5**: Components of a nucleotide and the possible nitrogenous bases

### 2.2.1.2 Secondary Structure

DNA found in nature is almost always found in a double-stranded fashion (as double-stranded DNA, dsDNA). Hydrogen bonding between matching bases (adenine with thymine, and guanine with cytosine, termed Watson-Crick base pairs) and the base-stacking from the parallel π-bonds from sequential base pairs provide a very stable structure in the form of a double helix.[45] This double helix can be considered rigid rod for short sequence pairs. The double helix can be unwound in the presence of DNA helicase or high temperatures, which can split the strands and cause them to separate. The threshold temperature for this to occur is called the melting temperature; this threshold is length- and sequence-dependent. Once melted, the two resultant single-stranded DNA (ssDNA) are comparatively flexible. If the temperature is returned to below the melting temperature, the two strands will re-hybridize, reforming the stable double helix structure.

Watson-Crick base pairing does not have to take place on separate strands. It is possible for a single strand with the necessary complementary sequence to loop back on itself and form base pairs; the complementary portion forms a duplex while the sequence in between forms the "hairpin" structure.[46] Structures like this can be useful when used as a molecular beacon, as a fully complementary strand can break the hairpin structure and hybridize with the entire sequence.

Structures beyond the typical Watson-Crick base pairs exist, which can give three-dimensional structures beyond a double-helical structure. One such structure is the G-quadruplex;[47] four planar guanine bases can associate by each contributing two hydrogen bonds and producing a tetramer structure. This tetramer is fairly strong and has limited interaction even with complementary cytosine strands. Two or more tetramers can π-stack on each other and create the structure known as the G-quadruplex. The G-quadruplex can be formed by a single strand weaving back and forth in various patterns,[48] or can be made by multiple strands (Figure 2.6). The strands themselves can run in a parallel or antiparallel fashion; this is largely determined by the polarities of the backbone and less so on whether or not they are part of the same sequence.[47] The parallel-antiparallel alignment also necessitate the *syn* or *anti* rotation of the base itself for proper hydrogen bond formation.[49] The remarkably stable structure has once been described as "a structure in search of functions", as it did not appear to have corresponding proteins that can assemble and disassemble such structures, but these have since been found in placental tissue and in certain tumour cells.[50,51]

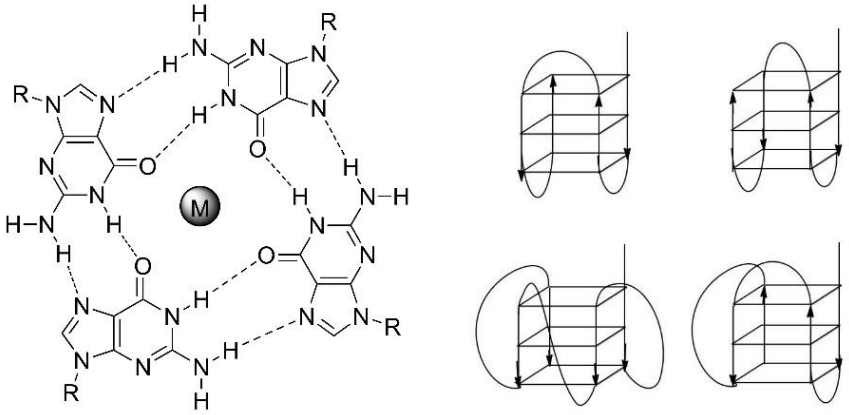


**Figure 2.6**: Structure of a guanine tetramer and different G-quadruplexes folded from a single strand.[48] Reprinted with attribution from: http://www.intechopen.com/books/oncogene-and-cancer-from-bench-to-clinic/structure-based-approaches-targeting-oncogene-promoter-g-quadruplexes

### 2.2.2 Isolation Techniques

To fully utilize DNA, one must be able to isolate and purify it from other materials. Several methods exist, all with varying degrees of efficacy and simplicity. The most commonly used method involves the addition of sodium salt (typically sodium acetate for pH control) and ethanol, incubation at −20°C overnight, followed by high-speed centrifugation of the now-insoluble DNA.[52] Approximately 60% recovery can be obtained for amounts as low as 0.6 ng, with improvements in yield coming from recovering DNA amounts greater than 100 ng or by increasing centrifugation time. Ethanol can be replaced with isopropanol, which is more efficient but more difficult to remove due to lower solvent volatility.

Smaller amounts or shorter strands of DNA can be recovered with the aid of co-precipitating carriers such as linear polyacrylamide or glycogen.[53,54] These carriers are able to non-covalently bind with DNA and share the property of insolubility in ethanol. Picogram amounts of DNA can be recovered with the assistance of these carriers. It is found that as a carrier, glycogen outperforms others in terms of overall recovery,[55] but commercial stocks of glycogen may have DNA impurities inside, possibly from bacterial origin.[56] Thus, polyacrylamide-assisted precipitation may be favoured.

### 2.2.3 DNA Aptamers and Cell Targeting

Aside from use as a genetic storage material, the properties of DNA also allow it to be used as aptamers. Aptamers are short single-stranded sequences with very high specificity of binding to a target analyte. Although aptamers exist in nature (*e.g.* riboswitches),[57] most are synthetically created and selected through systematic evolution of ligands by exponential enrichment (SELEX).[58,59] This method introduces a library of DNA sequences to a target analyte for binding. Sequences that exhibit strong binding affinities to the target are isolated from the non-binding sequences and amplified using PCR, then re-introduced to the analyte. After 15-20 iterations, a sequence with extremely high binding affinity will remain as the aptamer gained through selection. Aptamers are similar to antibodies in that they bind with high specificity, but have any advantages beyond this: They are much more stable than peptide-based antibodies with a longer shelf life, exhibit little to no batch-to-batch variation, and can function in non-physiological conditions.[4] In addition, they are not limited to immunologically active targets; inorganic analytes can also have a specific aptamer bind to it with high specificity. Aptamers have been

found for a wide variety of analytes, including adenosine,[60] cocaine,[61] caffeine,[62] mercury,[63] thrombin,[64] and vascular endothelial growth factor.[65]

Aptamer selection can be run on entire cells as well. This version of SELEX, known as cell SELEX, introduces the whole cell as a target for aptamer selection.[66] Intimate knowledge of the cell surface and its structural components is not required; any exposed component of the cell membrane is a potential target. In addition, targets will be in their native environment rather than isolated and potentially in an unnatural folding pattern.

#### 2.2.3.1 AS1411

A specific aptamer was found to have anticancer potential after binding to cancer cells. Named AS1411, this aptamer was surprisingly not discovered with intent; the original intent of the project that resulted in the discovery of this sequence was to elucidate triplex-forming oligonucleotides for modulating gene expression. However, while exploring control sequences, the sequence 5′-GGTGGTGGTGGTTGTGGTGGTGGTGG-3′ was found to have anticancer activity after binding to the cancer biomarker nucleolin,[67] and thus was given the name AGRO100 before being changed again to AS1411, and explored for further application. Although the aptamer has now been renamed yet again to ACT-GRO-777 after its acquisition from Antisoma by Advanced Cancer Therapeutics,[68] most literature continue to refer to the sequence as AS1411, and will be done so here as well.

The AS1411 aptamer is a G-rich oligonucleotide that forms a G-quadruplex secondary structure, giving it remarkable stability in physiological situations. Such G-quadruplex structures are found to have good affinity for nucleolin,[69,70] which is heavily expressed in cancerous cells as part of several oncological pathways and a marker for poor prognosis of health.[71] Once AS1411 binds with nucleolin, it additionally interferes with nuclear factor-κB essential modulator (NEMO),[69] which protects cells from apoptosis and is linked to developed resistances to chemotherapy in cancer cells.[72]

Despite its high affinity for nucleolin, its mode of action does not actually require nucleolin to be expressed on the cell membrane for cell uptake. Instead of the typical receptor-mediated endocytosis typical for uptake of drugs, AS1411 is taken in through macropinocytosis, independent of the presence of nucleolin. This induces hyperstimulation of further macropinocytosis, of which the pathway is now nucleolin-dependent.[73] Once inside the cell, the exact mechanism which AS1411 causes cell death is uncertain; one theory is that the binding of

AS1411 to nucleolin inside the cell prevents nucleolin from performing its other functions. Although nucleolin has many functions, one notable function is the stabilization of the *bcl-2* messenger ribonucleic acid (mRNA), required for the coding of the anti-apoptotic *bcl-2* protein. By competitively binding with nucleolin, AS1411 can strip *bcl-2* mRNA of its stabilizing protein, thus downregulating *bcl-2* and causing the cell to undergo apoptosis.[74]

Although AS1411 has shown a therapeutic effect on cancer cells, most research focus is directed on using it as a targeting ligand only. The AS1411 sequence has been shown to be successfully attached to various nanoparticles of different materials, including silica, phosphatidylcholine liposomes, and poly(lactic-co-glycolic acid)-co-poly(ethylene glycol) (PLGA-PEG).[75–78] In these cases, AS1411 is used as a ligand used to interact with the cancer cells only, while the nanoparticle contains a different payload with a therapeutic effect (Figure 2.7). Typically, these formulations contain multiple components and become complicated particles, and require organic solvents or other components that may be harmful in the body in order to synthesize them.[75,77–79]

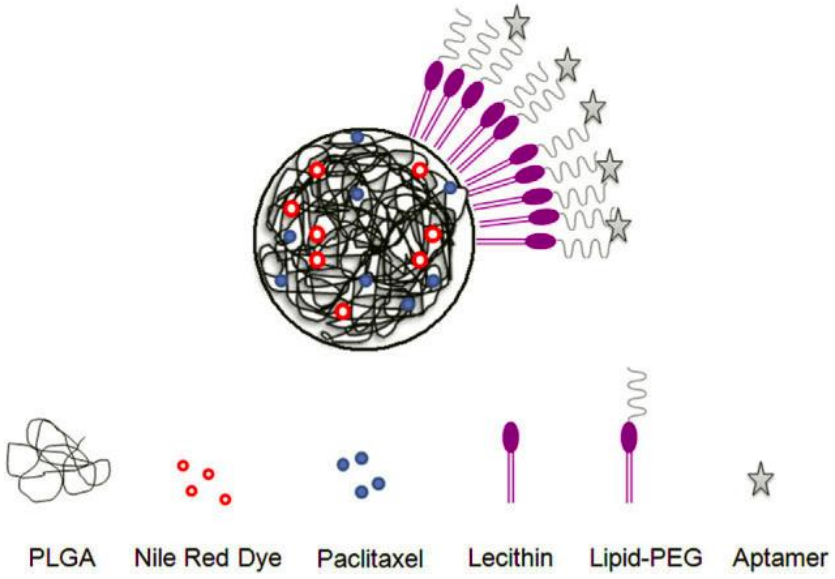


**Figure 2.7**: An example of a drug-loaded nanoparticle with AS1411 used for targeting.[78] The core of the nanoparticle is made using poly(lactic-co-glycolic acid), and encapsulates both a paclitaxel drug payload Nile Red Dye for identification. The outer surface is functionalized with lecithin, poly(ethylene glycol) and finally with AS1411 for targeting. Reprinted with permission.

## 3.0 DNA WITH STARCH CO-PRECIPITANT

The concept that starch nanoparticles could be used as a co-precipitant for DNA was accidently discovered while attempting covalent DNA conjugation. Since it has potential applications and may also tell us about the interaction between DNA and starch, a detailed characterization has been carried out on this topic. Although starch is typically found in its native granule format, EcoSynthetix (Burlington, Ontario) has been able to extrude starch to produce starch nanoparticles in the sub-micron range, much smaller dimensions than native granules can provide. As such, the option of using starch nanoparticle as a delivery vehicle for the delivery of chemotherapy drugs was explored, using aptamers such as AS1411 as a targeting ligand. Originally, the intention was to have DNA covalently attached to starch directly using EDC-NHS coupling. However, during the optimization of the protocol for sample purification, it was found that DNA would precipitate out of solution along with the starch even with no coupling agents present. We decided to explore this phenomenon to see if we could use it for any practical purposes.

EcoSynthetix has provided different grades of starch nanoparticles with various degrees of crosslinking using their proprietary crosslinking agent. These EcoSynthetix nanoparticles (ENP) came in different formulations, named GX0.0, GX1.0, GX3.0, and GX5.0 based on their crosslinking content (*i.e.* crosslinking agent concentrations from 0% to 5% by weight). The particles were used to determine which formulation had the best efficacy in DNA precipitation.

### 3.1 Rationale

DNA precipitation is an important part of any protocol that requires the purification of DNA from a solution containing other materials. Traditional DNA purification techniques exist that can be moderately effective for separating DNA from cell lysate. However, the technique is not as effective when isolating shorter oligonucleotides at lower concentrations, such as for use as an oligonucleotide-based sensor or for functionalizing nanoparticles. The use of a co-precipitant is one method of further increasing the effectiveness of current DNA purification methods. With a co-precipitant, the DNA would adsorb onto the surface of an additional insoluble material, and together would precipitate out of solution. However, there are still limitations using these methods that need to be addressed. For example, the use of glycogen as a co-precipitant has shown success in precipitating small amounts of DNA,[54,55] but commercial samples of glycogen

have been found to contain trace amounts of DNA contaminants.[56] Linear polyacrylamide is an alternative co-precipitant, but requires additional steps in polymerization, and residual unpolymerized acrylamide may raise toxicity concerns depending on the end use of the DNA.

The use of starch as a co-precipitant has several advantages over the aforementioned agents. Starch is much less costly than glycogen or polyacrylamide, and the protocol for precipitation is much simpler; while the use of other co-precipitants typically requires overnight incubation with refrigeration, using starch nanoparticles can allow incubation in ambient conditions for only an hour.

## 3.2 Theorized Limit of Detection

To determine the effectiveness of using starch as a precipitant, various solutions and dispersions were prepared and mixed together and allowed to incubate before centrifugation. A DNA solution was prepared using a 12-base ssDNA labeled with 6-carboxyfluorescein (FAM) DNA (5′-FAM-CACTGACCTGGG-3′) at 50 µM in 100 mM 4-(2-hydroxyethyl)-1-piperazineethanesulfonic acid (HEPES) buffer at pH 7.6. Starch dispersions with each of the formulations were prepared at 10% w/v in Milli-Q water, and serially diluted for lower concentrations. A working buffer solution of 50 mM 2-(N-morpholino)ethanesulfonic acid (MES) buffer and 50 mM NaCl at pH 6.0 was also prepared.

To allow DNA and starch to interact, mixtures were created with 2 µL DNA solution, 2 µL starch dispersion, and 16 µL MES/NaCl buffer, then stored in the dark for 1 hour. To precipitate out the DNA and starch, 40 µL of ethanol was added, and the mixture was then centrifuged at 15000 RPM for 20 minutes. To determine the amount of precipitated DNA, fluorescence measurements were taken from the supernatant, while the resultant precipitant from centrifugation was left undisturbed. 5 µL of the supernatant was removed and added to 95 µL of 50 mM HEPES buffer. Fluorescence measurements were taken by a plate reader at 485 nm excitation and 525 nm emission with an average of 4 readings performed. As supernatant fluorescence can only come from free FAM-labeled DNA, the fluorescence reading in the supernatant was negatively correlated with DNA adsorption onto starch. As controls, fluorescence readings of free DNA with and without the addition of ethanol were measured for comparison. It was found that 0.1% w/v starch is enough to precipitate out over 90% of DNA present, despite the much shorter length of oligonucleotides used (Figure 3.1).

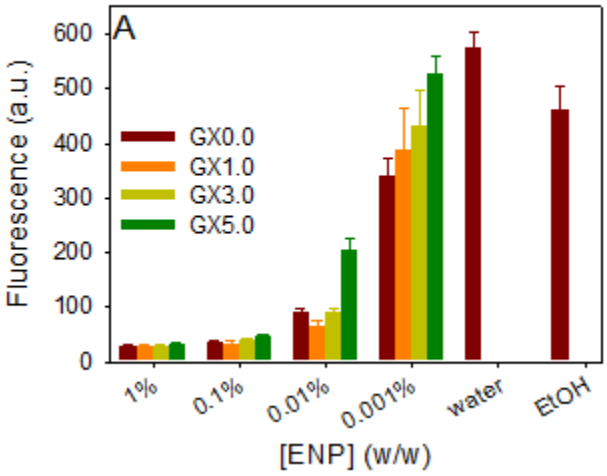


**Figure 3.1**: Supernatant fluorescence of starch used to precipitate out FAM-labeled 12 base DNA. Note that the controls for free DNA and DNA with ethanol are by themselves because although they are labeled as GX0.0, there is actually no starch present in their respective mixtures.

### 3.3 Effect of Crosslinking Density

Crosslinking density in polymeric nanoparticles is typically associated with a stiffer particle that is less porous and less prone to deformation. The additional material can have one of two effects; the additional material can enlarge the particle, but the crosslinks can also prevent particle swelling when in aqueous solutions.[80] It can be seen that higher amounts of crosslinks discourages DNA interaction with starch (Figure 3.1). This particular relation is not yet understood, but one hypothesis is that crosslinks reduce the amount of surface area available for DNA to interact with. As GX0.0 appears to have the best interaction with DNA, subsequent experiments will use only this formulation, and at 0.1% w/v concentration.

### 3.4 Effect of Alcohol Concentration

It is known that ethanol can precipitate out DNA by causing salt cations to re-associate with its phosphate backbone, minimizing charge repulsion and inducing aggregation.[81] To confirm this, progressively higher amounts of ethanol or isopropanol, another possible precipitating solvent, was added, and fluorescence measured (Figure 3.2). It can be seen that the higher concentration of alcohol that was added, the more starch and DNA was able to be co-precipitated, as shown by the reduced fluorescence signal in the solution supernatant.

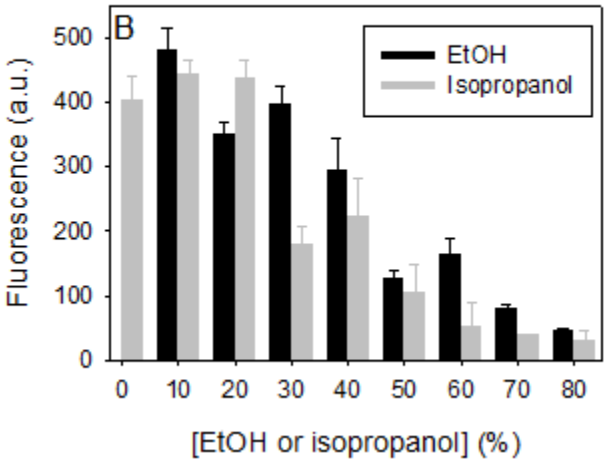


**Figure 3.2**: Effect of varying alcohol concentrations on starch precipitation.

It can be seen that as a general trend, the increase of alcohol concentration improves the precipitation efficiency of the GX0.0 starch nanoparticle. The effectiveness begins to flatten off between 60% and 70% for both ethanol and isopropanol, confirming the use of double volume alcohol during the precipitation protocol; while increasing the alcohol concentration can further increase DNA recovery, the nearly 90% recovery seen should be sufficient unless the additional recovery is warranted. Also, although it is apparent that isopropanol outperforms ethanol in DNA precipitation, previous protocols of DNA precipitation feature the use of ethanol, and therefore the use of ethanol will be continued for these studies.

### 3.5 Effect of DNA Lengths

The ability to precipitate short ssDNA oligonucleotides is surprisingly effective. However, we decided to explore the effectiveness of precipitating DNA of different lengths. The experiment was repeated with FAM-labeled 15A (15 consecutive adenosine nucleotides), 30A, 45A, and 90A each introduced to GX0.0 and allowed to incubate for an hour, then centrifuged with twice the volume in ethanol. The fluorescence readings of the resulting supernatant show no significant difference in efficacy of precipitating out oligonucleotide chains regardless of the investigated lengths (Figure 3.3).

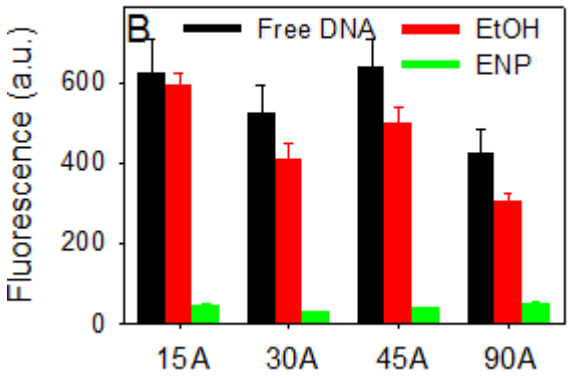


**Figure 3.3**: Effect of varying oligonucleotide length on starch precipitation.

### 3.6 Effect of DNA Bases

Next we examined the effects of using different nucleobases to see if the DNA adsorption is base-specific. The experiment was repeated with FAM-labeled 15A, 15T, 15C and 15G, each representing the 4 basic nucleotides (*i.e.* adenine, thymine, cytosine, and guanine), after incubating with GX0.0 for 1 hour, then centrifuging with twice the ethanol volume (Figure 3.4). Again, there was no notable difference between the oligonucleotides in binding once introduced to GX0.0. It should be noted that the controls with free DNA and ethanol have greatly reduced fluorescence for 15G. This is expected, as guanine is a known fluorescence quencher,[82,83] and a reduction in fluorescence signal would be likely for all fluorescent samples containing guanine.

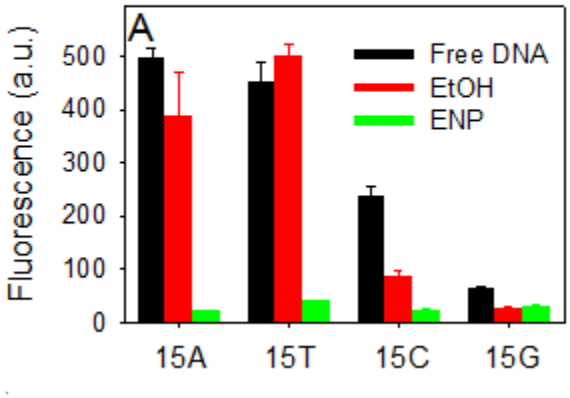


**Figure 3.4**: Effect of varying nucleobases on starch precipitation.

### 3.7 Effect of Salt and pH

Traditionally, salt concentration is an important parameter for the ethanol precipitation of DNA. Specifically, the low dielectric constant in ethanol will allow cations in salt to associate with polyanionic DNA, effectively neutralizing its charge and reducing its solubility. To test this, magnesium was added as a divalent cation through the addition of magnesium chloride to the solution. Magnesium chloride concentrations were prepared through tenfold serial dilution from 1 M to 1 mM $MgCl_2$. Samples were prepared as previously described with GX0.0, with 2 µL of $MgCl_2$ solution added in, effectively dilution the $Mg^{2+}$ concentration by 10. Samples were then incubated with 1 hour under ambient conditions. The samples were then centrifuged, and 5 µL of the supernatant removed and placed into 95 µL of HEPES buffer for fluorescence analysis (Figure 3.5A). Although the addition of $Mg^{2+}$ appears to have improved the precipitation slightly, the difference is not pronounced compared to precipitating without the use of magnesium salts at all.

The effect of pH on precipitation was also investigated. Using pH 3 and 9 as an arbitrary "high" and "low" pH relative to the pH of MES at 6, a citrate buffer was prepared at pH 3, and used in place of the MES buffer in precipitating out DNA via GX0.0. As a pH 9 buffer was not readily available, a suitable replacement was made by titrating MES to pH 9 using dilute NaOH. The precipitation was then repeated using these pH solutions (Figure 3.5B). At both pH ranges, there is no noticeable difference in precipitation efficacy.

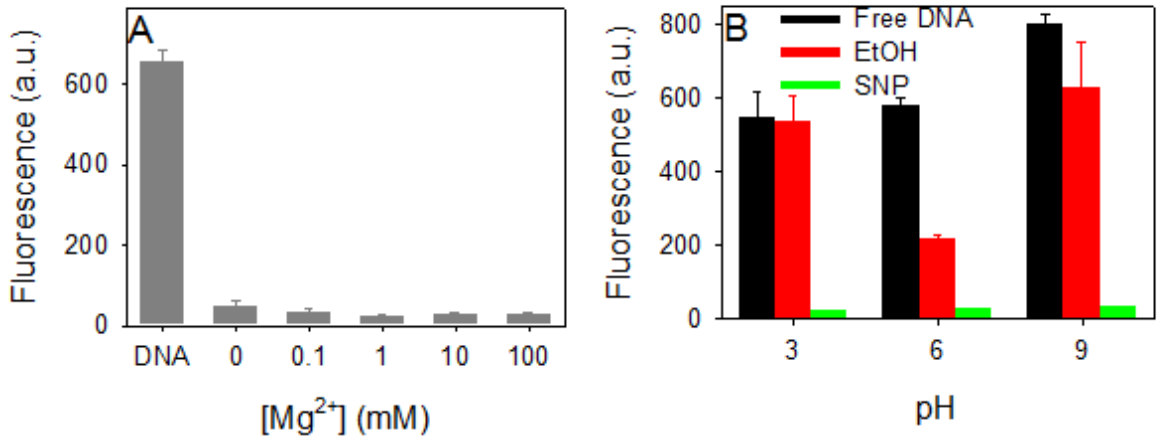


**Figure 3.5**: Effect of **A**) $Mg^{2+}$ and **B**) pH on starch precipitation.

### 3.8 Effect of ssDNA and dsDNA

The ENPs were shown to precipitate out a wide variety of ssDNA with high recovery; the ability for ENPs to precipitate dsDNA was then investigated. To investigate this, polyacrylamide gel electrophoresis (PAGE) was used to analyze a library of several low molecular weight DNA lengths simultaneously, ranging from 25 to 766 base pairs (bp). Samples were prepared the same way by incubating with GX0.0 for 1 hour under ambient conditions. Twice the volume of ethanol was then added and the samples centrifuged. The supernatant was removed and the remaining pellet resuspended in water. A 15% acrylamide/bis-acrylamide (29:1) solution was casted into a gel with ammonium persulfate and tetramethylethylenediamine (TEMED) as initiator and catalyst, respectively. Both the supernatant and resuspended starch pellet were loaded into the gel with 30% glycerol. The gel was allowed to run with a tris-borate-ethylenediaminetetraacetic acid (EDTA) buffer (collectively TBE buffer) for 90 minutes at 600 V and 100 mA to ensure good separation of DNA lengths, then stained for 15 min. with ethidium bromide. A fluorescence image was taken at 302 nm excitation and 580 nm emission (Figure 3.6).

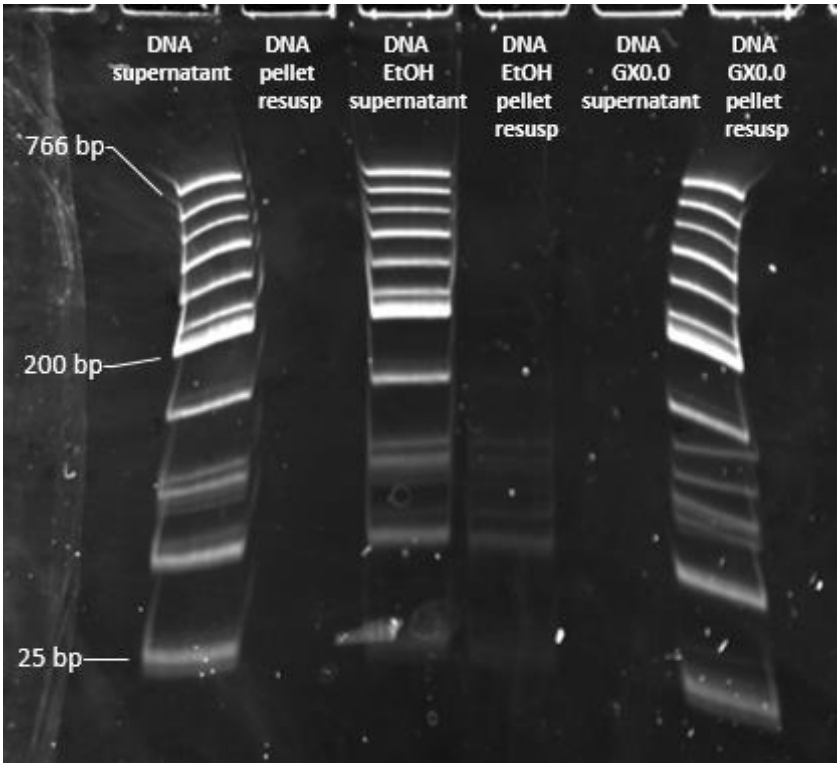


**Figure 3.6**: PAGE results of double-stranded DNA precipitated out with starch

From the results, all bands for the GX0.0-treated sample are strongly present in the resuspended pellet, with no visible bands remaining in the supernatant, while the reverse is true in the controls. The GX0.0 ENP was successful at precipitating out DNA lengths along the entire length of the ladder, showing good generalizability for precipitation. The quality of the bands appears less than optimal; this is possibly due to the residual ethanol in the supernatant solutions which can affect the quality of the electrophoresis.

### 3.9 DNA Recovery from Starch

While DNA can be recovered from starch through PAGE, an alternative method was explored through the degradation of the starch in GX0.0 using α-amylase. As the ENPs are all made of mostly starch, it was expected that the nanoparticles can still be degraded by α-amylase. To test for this, the iodine test was used; iodine is a well-established method used to establish the presence of starch.[84–86] Various iodide-iodide complexes are able to position itself inside the double helical structure of amylose, inducing a colour change that can be tracked as a rise in absorbance at 580 nm. The loss of the double helical structure (*e.g.* through digestion by α-amylase) would remove the resulting colour, and the corresponding absorbance at 580 nm would drop. To test this, starch nanoparticles were incubated with α-amylase at 37°C for 60 minutes, and iodine was added after. A UV-Vis spectrum was obtained from 200 to 1100 nm wavelength. A drop in absorbance at 580 nm can be seen, indicating a loss of helical structure that follows the degradation of the amylose content (Figure 3.7). Note that other peaks are present, such as at 290 nm and 350 nm, but the largest change by far can be observed in the 580-620 nm region as reported in previous work by other groups.

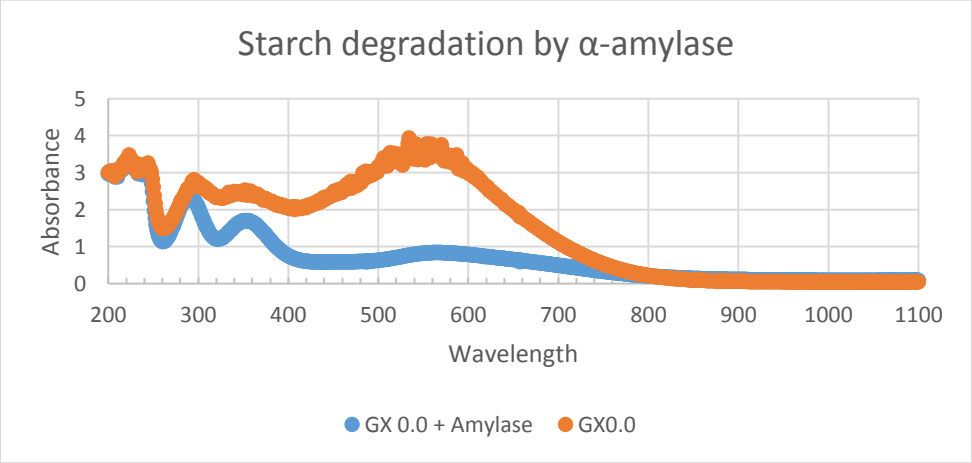


**Figure 3.7**: Digestion of starch nanoparticle by α-amylase

Next we investigated if the starch can be degraded by α-amylase after DNA adsorption. It is possible that additional crosslinking or adsorption of DNA onto the surface of ENPs may render the α-1,4 glycosidic bonds inaccessible for amylase. The precipitation protocol was run again by incubating the various grades of ENPs for 1 hour. In parallel, dextrin was also run as a positive control, and dextran was run as a negative control. Samples were then incubated with α-amylase at 37°C for 1 hour, then supplemented with twice the volume of ethanol and centrifuged. The pellet was photographed under blue light and filter to isolate the green fluorescence (Figure 3.8). In dextrin and all starch-based samples, the amylase present in the indicated hydrolyzed the α-1,4 glycosidic bonds in the polysaccharides, producing more soluble oligosaccharides that did not pelletize, compared to all samples without amylase, which pelletize properly. However in the case of dextran, the α-1,6 glycosidic bonds in this polysaccharides were not cleavable by α-amylase, and the pellet remained largely intact for both samples regardless of the presence of amylase.

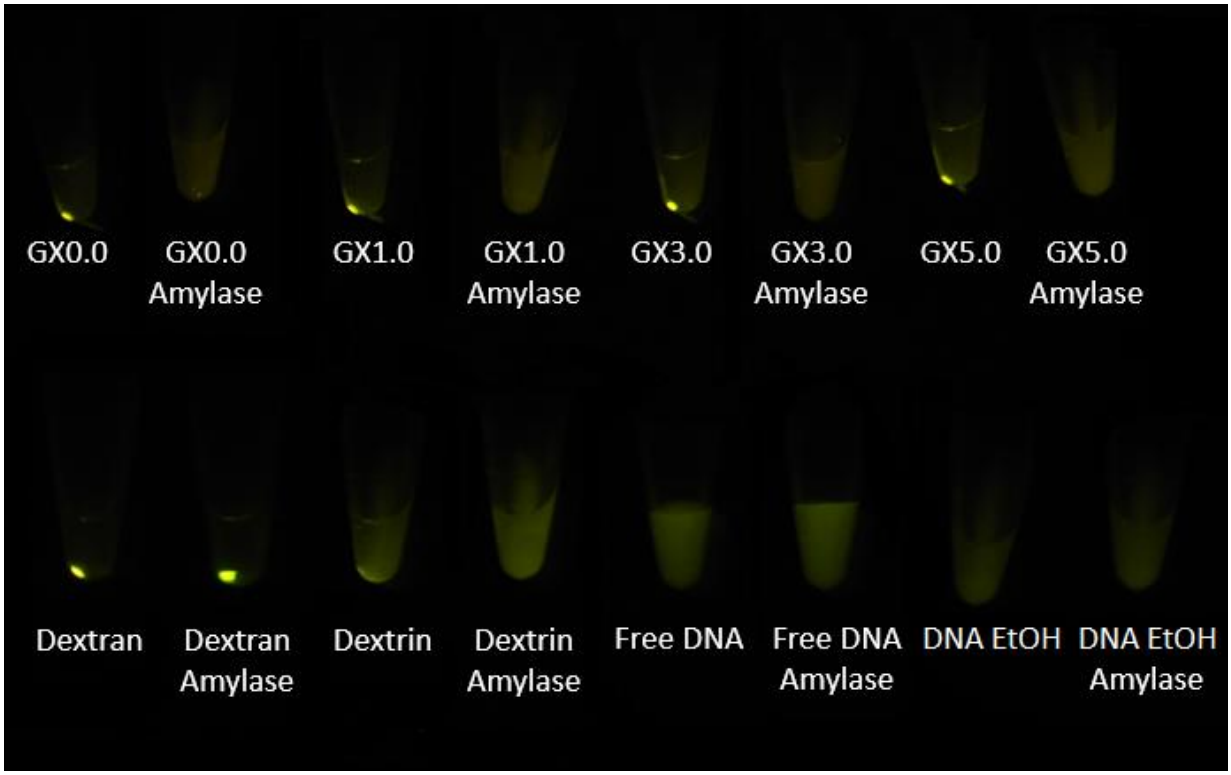


**Figure 3.8**: Digestion of various oligosaccharides by α-amylase

### 3.10 Comparisons against Other Isolation Techniques

The use of starch as a co-precipitant for DNA confers many advantages not available to the standard precipitation protocol. The first would be that the precipitation protocol is greatly reduced in both complexity and time; ethanol precipitation with starch nanoparticles as a co-precipitant can occur in ambient conditions without the need for –20°C refrigeration. In addition, for the precipitation of short oligonucleotides, standard protocol suggests incubation to take place overnight.[52,53] The use of starch nanoparticles can allow precipitation to occur in the same time frame, thus shortening the precipitation protocol greatly. Finally, the cost of starch is significantly lower than an equivalent amount of acrylamide or glycogen, allowing DNA precipitation to be improved at a relatively low cost.

Starch necessarily should be in nanoparticle form before it is used for precipitation. Native starch granules are rather large particles, and typically will not disperse in water thoroughly enough to effectively co-precipitate DNA. The granules will typically settle out of solution before the 1 hour has elapsed for the protocol, thus making it difficult to effectively co-precipitate DNA.

### 3.11 Materials and Methods

Starch nanoparticles (GX0.0, GX1.0, GX3.0, and GX5.0) were graciously provided by EcoSynthetix Inc. (Hamilton, Ontario). Dextrin (from corn, commercial grade, Type II), dextran (from *Leuconostoc* spp.), iodine, potassium iodide, and sulfuric acid were purchased from Sigma-Aldrich (St. Louis, Missouri). HEPES, MES, NaCl, and $MgCl_2$ salts, along with citric acid, sodium hydroxide, and ethidium bromide were purchased from Mandel Scientific (Guelph, Ontario). The various DNA sequences (12-mer, 15A, 30A, 45A, 90A, 15T, 15C, 15G) were purchased from Integrated DNA Technologies (Coralville, Iowa). The Low Molecular Weight DNA Ladder (N3233S) was purchased from New England Biolabs Ltd. (Whitby, Ontario). Ammonium persulfate, TEMED, TBE buffer, and acrylamide/bis-acrylamide (40% solution, 29:1) were purchased from Bio Basic Canada (Markham, Ontario). Iodine, potassium iodine, and α-amylase were purchased from Sigma-Aldrich. Glycerol was purchased from Merck (Gibbstown, New Jersey).

### 3.11.1 Production of Nanocrystalline Cellulose.

Nanocrystalline cellulose was produced following the protocol of described by Saïd Azizi Samir *et al*.[87] with slight modification. A 65 wt% solution of sulfuric acid was prepared by addition into water and the temperature raised to 40°C under stirring. Cellulose was collected from Whatman filter paper (Madstone, England) cut into small pieces and placed into the sulfuric acid solution for 35 min. Afterwards, the resulting NCCs were washed repeatedly through repeated centrifugation and resuspension until neutrality was reached, then dried and resuspended in known concentrations.

### 3.11.2 General DNA Precipitation with Starch

Stock solutions of 500 mM MES, 500 mM HEPES, and 3 M NaCl were first prepared. DNA solutions were prepared at 50 µM concentrations in 100 mM HEPES at pH 7.6. Starch nanoparticle dispersions were prepared at 10% w/v in Milli-Q water. Serial dilutions of 1:10 were sequentially prepared for lower concentrations. Buffer solutions were prepared with 50 mM MES and 50 mM NaCl at pH 6.0. DNA and starch interactions were prepared by mixing 2 µL DNA solution, 2 µL starch dispersion, and 16 µL MES/NaCl buffer. For larger volumes needed for digital photography, volumes were scaled up accordingly, *e.g.* 5 µL DNA solution, 5 µL starch dispersion, and 40 µL MES/NaCl buffer. The mixture was briefly vortexed to ensure good mixing, then allowed to sit in ambient temperature away from light for 60 min. Precipitation of DNA was performed by adding twice the solution volume of ethanol (*e.g.* 40 µL for a 20 µL solution, or 100 µL for a 50 µL solution) and centrifuged at 21000 RCF for 30 min. This number is approximate, as two centrifuges were available (Eppendorf Centrifuge 5430 R or 5424) with different centrifuge radii, and spins were set in RPM. For fluorescence readings, 5 µL was removed from the supernatant and added to 95 µL of 50 mM HEPES, then put onto a standard 96-well plate. Fluorescence readings were performed on a SpectraMax M3 from Molecular Devices, LLC (Sunnyvale, California) at 485 nm excitation and 525 nm emission. Each sample had 4 wells, and each well was read with 6 flashes of light.

This protocol was used for determining the limit of detection using the starch nanoparticles, for determining the effect of crosslinking density on precipitation efficacy, the effects of DNA length, and the effects of DNA sequence used.

### 3.11.3 DNA Precipitation with Varying Alcohol Concentration

Various solutions of water/alcohol mixtures (of ethanol or isopropanol) were prepared. These solutions of 80 µL consisted of increasing ethanol percentage (*e.g.* 80 µL water/0 µL alcohol, 70 µL water/10 µL alcohol, 60 µL water/20 µL alcohol, etc.), with 9 mixtures of ethanol and 9 mixtures of isopropanol made. One mixture of 80 µL water was discarded due to redundancy.

The general DNA precipitation protocol was followed using only GX0.0 for sample volumes of 20 µL, with duplicates made for each water/alcohol mixture. The water/alcohol mixture was added to the 20 µL after 1 hour incubation for a total sample volume of 100 µL, then centrifuged. From here the protocol proceeded as normal, with centrifugation and removal of a portion of the supernatant for fluorescence readings as described in the original precipitation protocol.

### 3.11.4 DNA Precipitation with Additional $Mg^{2+}$

A solution of 1 M $MgCl_2$ was prepared and serially diluted tenfold to 100 mM, 10 mM and 1 mM. Samples were prepared as previously described for a 20 µL sample size, except 2 µL of the prepared magnesium solutions were added in, resulting in 100 mM, 10 mM, 1 mM, and 0.1 mM $Mg^{2+}$ concentrations, respectively. An additional 2 µL of Milli-Q water was added into both free DNA and DNA/GX0.0 with no $Mg^{2+}$ controls to maintain concentration differences. From here the protocol proceeded normally, with centrifugation and fluorescence readings obtained in a similar manner described above.

### 3.11.5 DNA Precipitation with varying pH

A 500 mM citric acid/sodium citrate solution was titrated down to pH 3 with dilute hydrochloric acid and monitored using a pH meter, and sodium chloride added to a final concentration of 50 mM. Because of a lack of basic buffers available, the stock MES/NaCl buffer was simply titrated to pH 9 using dilute sodium hydroxide solution and monitored using a pH meter.

The general protocol mentioned was followed for preparing samples, except the 50 mM MES/50 mM NaCl buffer solution was replaced with the pH 3 and pH 9 solutions for their respective samples. The protocol was unaltered for pH 6, as this was the original pH of the MES buffer. From there on the protocol proceeded normally, with centrifugation and fluorescence readings obtained in a similar manner described in the original protocol.

### 3.11.6 Precipitation of Double-Stranded DNA Ladder

Polyacrylamide gel electrophoresis was performed on a 15% acrylamide/bis-acrylamide gel. A 250 mL stock solution of 15% acrylamide/bis-acrylamide was created by adding 156.25 mL of Milli-Q water to 93.75 mL of 40% acrylamide/bis-acrylamide. For casting acrylamide gel, 22 mL of the 15% solution was added to a volumetric flask along with 50 mL of 10% w/w aqueous ammonium persulfate as initiator and 20 mL of TEMED as catalyst. Gel casting equipment was obtained from C.B.S. Scientific (Del Mar, California). Gels were cast for 90 minutes to allow polymerization to proceed and form wells for loading samples. Wells were rinsed with TBE buffer before the addition of samples. Electrophoresis of the DNA ladder was prepared having the ladder proceed through the general precipitation protocol. The supernatant was separated from the pelletized starch/adsorbed DNA, and the pellet resuspended in 20 µL 50 mM HEPES. The resuspended pellet and 20 µL of the supernatant were each mixed with 20 µL of 30% w/w of glycerol and loaded into their respective loading wells within the polyacrylamide gel. The gel electrophoresis was performed at 600 V and 100 mA for 90 minutes using a 2060P power supply from Thermo Scientific (Waltham, Massachusetts). The resultant DNA migration inside the gel was stained with 0.5 µg/mL of ethidium bromide for 30 min. Fluorescence images of the stained gel was obtained at 302 nm excitation and 580 nm emission using a Gel-Doc Universal Hood III from Bio-Rad Life Sciences (Mississauga, Ontario).

### 3.11.7 Iodide Staining and Amylase Digestion

Iodine solutions were prepared fresh with 0.1% w/w iodine and 1% w/w potassium iodide. 2 µL of the solution was added to the starch formulation and colour was allowed to develop over a few seconds, then mixed to ensure homogeneity. UV-Vis readings performed on an 8493 UV-Vis spectrophotometer from Agilent Technologies Canada (Mississauga, Ontario).

Digestion of starch by α-amylase was done similar to the general precipitation protocol described above; the major change is the addition of 5 µL of 2 mg/mL α-amylase after incubation of 1 hour in ambient conditions. The α-amylase was allowed to incubate for an additional 60 minutes at 37°C before the addition of ethanol and subsequent centrifugation. Photographs were taken using a Canon PowerShot SD1200 IS digital camera using an Invitrogen (Carlsbad, California) Safe Imager 2.0 for lighting.

## 3.12 Conclusions and Future Directions

It has been found that the starch nanoparticles, especially the GX0.0 formulation, possess a strong ability to co-precipitate DNA by taking advantage of their insolubility in ethanol. The precipitation conditions are much more simplified compared to standard protocols, with a lower associated cost. This interaction is applicable to a wide variety of DNA types, irrespective of length or sequence, and can be used for both ssDNA and dsDNA. In addition, a high salt concentration is not necessary, nor would pH conditions alter its efficacy.

Future work can attempt to determine the cause of interactions between the two substances, such as studying its interaction in the absence of salt, monitoring fluorescence anisotropy, and attempting DNase cleavage of DNA while bound to starch nanoparticles. In addition, comparing starch nanoparticles to other established co-precipitants directly can quantify the advantage of using them in terms of cost and efficacy.

## 4.0 DNA COVALENTLY CONJUGATED ONTO STARCH

The interaction of DNA and starch is not limited to only physical adsorption. Both DNA and starch can be functionalized to allow a stronger, less transient interaction. This can allow the DNA-functionalized starch nanoparticle to retain its combined function in a wider variety of conditions, as well as providing a more predictable conformation for DNA. This is especially important in the case of aptamers, such that it can adopt the necessary configuration to bind to its target.

The use of starch as a drug delivery vehicle has obvious benefits, as starch is a well-known polysaccharide with well-established biocompatibility in humans. It is very commonly available in staple foods, and as such, the chance of immune rejection or pyrogenicity is extremely low. By loading a starch-based nanoparticle with anticancer drugs encapsulated within, it can make a simple yet efficient drug delivery system.

In addition to the various grades of ENPs, EcoSynthetix also has a "bulk" formulation which is currently already in use in the market as a paper binder. This formulation was used the majority of the oxidation and conjugation reactions, and simply labeled ENP rather than a specific formulation code.

### 4.1 Rationale

The idea of using starch as a drug delivery vehicle is an attractive idea due to the excellent biocompatibility of the vehicle. Starch-based nanoparticles have been previously used to deliver drugs such as indomethacin,[37] testosterone,[39] and cisplatin,[88] along with diagnostic agents such as magnetic nanoparticles.[89] A major drawback of these delivery systems is their particle sizes; being fairly complicated particles, their particle size typically ranges larger than 100 nm. This large size would make the nanoparticles prone to hepatic clearance, which would limit the amount of time spent in the body and be possibly cleared before it reached the tumour site. Although the exact clearance mechanism is more complex, it has been found that nanoparticles above 100 nm is likely to be cleared by the liver.[90] Conversely, particles that are too small, such as below an 8 nm threshold, may be cleared out by the kidney.[91,92] Therefore, having a nanoparticle in the size range of 10-100 nm is ideal to allow long circulation times and avoid both hepatic and renal clearance.

In addition, typical targeting mechanisms take advantage of the enhanced permeability and retention (EPR) effect found in the vasculature around tumour sites.[89,93] Solid tumours can experience explosive growth and would require nutrients to fuel this progression. To do so, it typically exhibits abnormally fast angiogenesis enabling hypervascularity, with high permeability to ensure nutrients can reach tumour sites in sufficient quantities.[94] This high permeability can also attract and sustain the presence of drug delivery nanoparticles, making it a feasible passive targeting system. Targeting via EPR can be supplemented with a more active targeting system, such as using receptor-mediated endocytosis.[95] Such active targeting would be done with the assistance of targeting ligands such as antibodies. A starch-based delivery vehicle will be introduced in the optimal size that maximizes circulation time to take advantage of both active and passive targeting to cancer cells, using the aptamer AS1411 to target membrane-bound nucleolin to assist in cell uptake.

## 4.2 TEMPO-mediated Starch Oxidation

The covalent linkage of DNA onto starch cannot be done in their native forms. Both DNA and starch must be modified with functional groups to allow for a successful coupling. There are many coupling mechanisms available; in order to limit particle size growth, functionalization should be kept as simple as possible with no intermediate linking agents. Amine-functionalized DNA is commercially available (*e.g.* from Integrated DNA Technologies), which is an ideal functional group for DNA coupling through an amide bond. This would necessitate the oxidation of hydroxyl groups in the anhydroglucose subunit into a carboxyl functional group.

The oxidation of starch hydroxyls can be done using multiple strategies. One option is to use 2,2,6,6-tetramethylpiperidine-1-oxyl (TEMPO) as a catalyst for the oxidation of primary hydroxyls.[96] In the anhydroglucose subunits, a primary hydroxyl can be found on the 6′ carbon, while the other hydroxyls present on the 2′ and 3′ carbons are both secondary. Using TEMPO can allow for selective oxidation of only the 6′ carbon from a hydroxyl into a carboxyl group.[97]

### 4.2.1 Theory

The oxidation of starch using TEMPO as a catalyst typically requires sodium bromide as a co-catalyst and sodium hypochlorite as an oxidizing agent. The reaction is typically done at pH 10-11 while maintaining temperature near 0°C. The oxidation can proceed twice on a 6′ carbon primary hydroxyl; the first oxidation will convert the hydroxyl group to an acetal group, while

the second oxidation will convert the acetal group into a carboxyl group via a hemiacetal intermediate (Figure 4.1).[98] The conversion reaction is limited by the amount of sodium hydroxide present, which is used both to maintain the high pH required for the reaction to proceed, and to convert the acetal into a hemiacetal intermediate for further oxidation into a carboxylic acid.

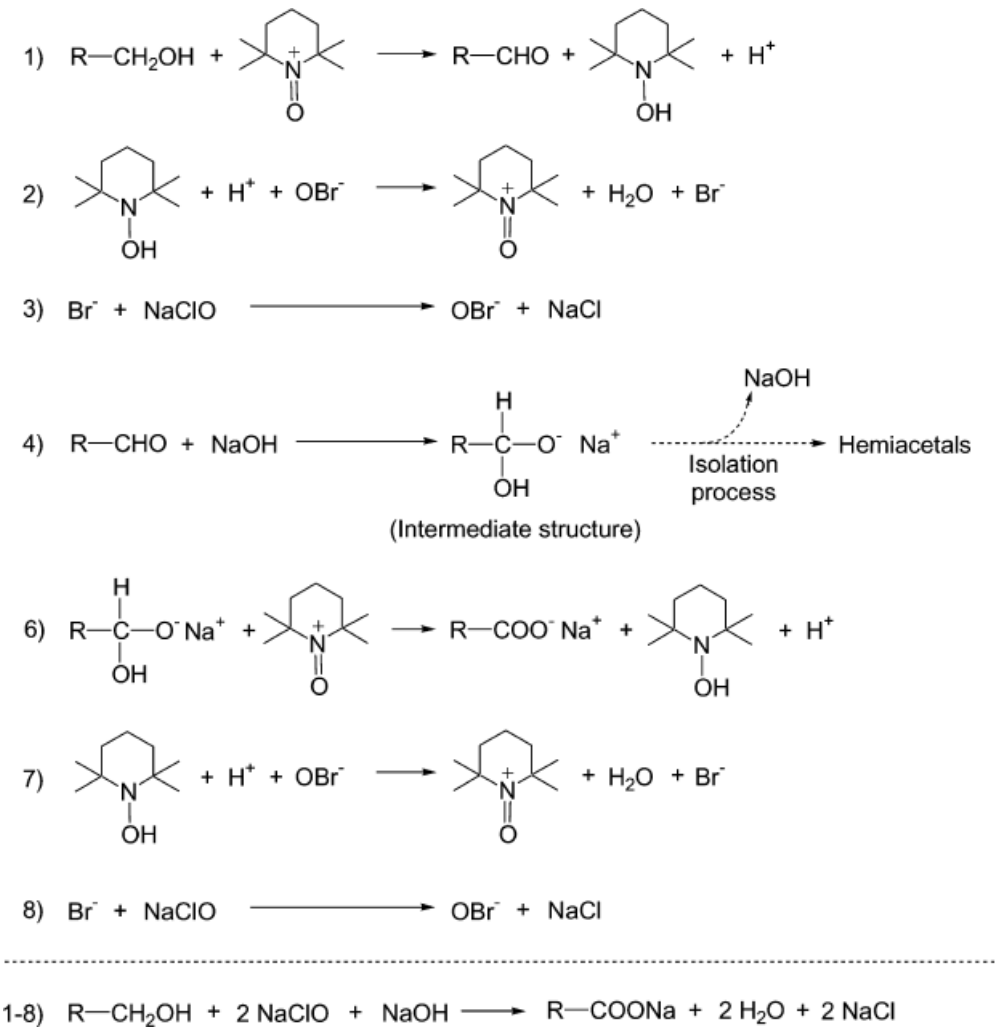


**Figure 4.1**: Proposed mechanism for a TEMPO-mediated oxidation reaction of a primary alcohol.[98] Reprinted with permission

A typical TEMPO oxidation proceeds as follows[98]: A solution of 5% ENPs is heated for 80°C for 30 min. TEMPO (0.01 molar ratio per anhydroglucose subunit) and NaBr (0.2 molar ratio per anhydroglucose unit) are dissolved separately while the starch solution is brought down

to under 5°C in an ice-water bath. The two solutions are added together and the pH of the solution is raised to above 10 using the addition of 0.5 M NaOH. A controlled amount of sodium hypochlorite is added to allow for incomplete oxidation of starch; the oxidation proceeds with a corresponding pH drop. To maintain a high pH above 10 necessary for the reaction to proceed, additional 0.5 M NaOH was added. The reaction was monitored until pH is stabilized. Further reaction was quenched by the addition of ethanol, and the ENPs were purified from unreacted reagents through multiple precipitations, centrifugations, and re-dispersions, before finally being lyophilized to remove any remaining solvents.

To confirm successful oxidation of the ENPs, dynamic light scattering and ζ-potential measurements was performed on them and compared to un-oxidized samples (Table 4.1). The particles showed good distribution in size, although some large micron-size aggregates were detected (Figure 4.2). Originally, a slightly larger particle was expected, due to the newly-oxidized portions of the nanoparticles experiencing charge repulsion and increasing the swell of the nanoparticles in water; however this is shown to not be the case. It is possible that the particles instead became smaller due to the depolymerisation of starch at high pH; it would mean that the depolymerisation is much more significant than anticipated. The measured ζ-potential, however, shows an apparent strong negative charge that would arise from successful conversion from hydroxyl groups to deprotonated carboxyl groups.

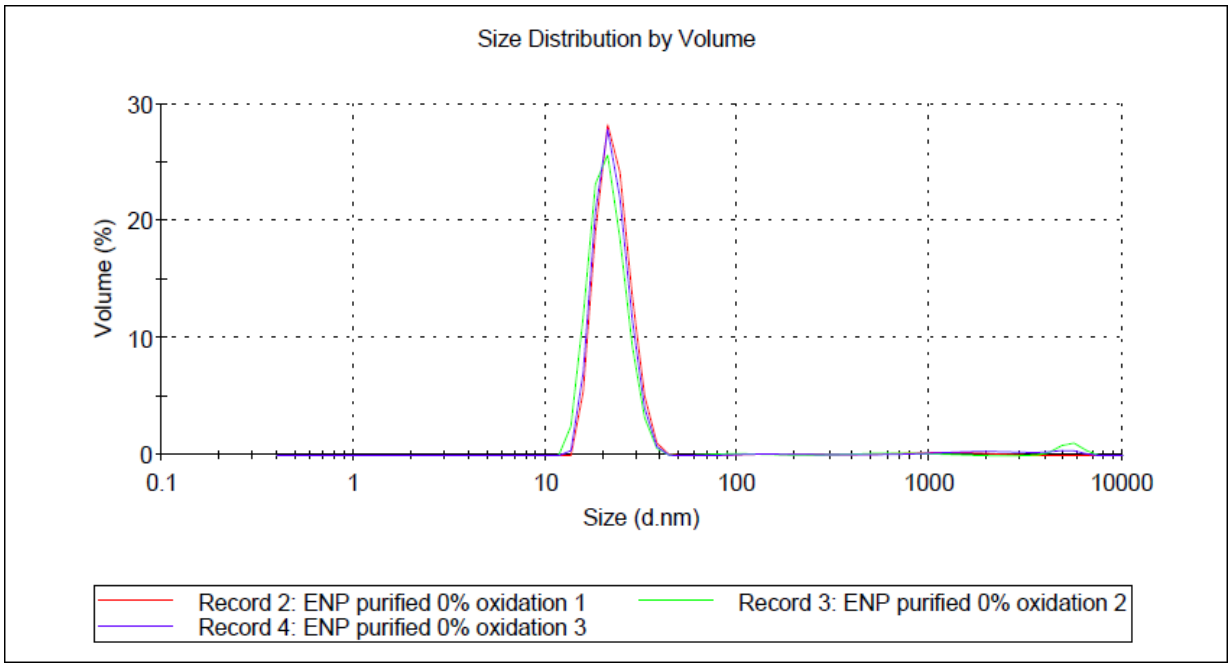


**Figure 4.2**: Sample dynamic light scattering spectrum by volume

**Table 4.1**: Dynamic Light Scattering and zeta potential measurements of oxidized ENPs

| Characteristic | ENP | ENP 20% COOH |
|---|---|---|
| D (nm) | 22.27 | 9.43 |
| ζ (mV) | 1.72 | -28.25 |

### 4.2.2 Removal of Glycerol

Previous formulations of ENPs provided by EcoSynthetix contained glycerol to be used as a plasticizer. This addition was for the use of ENPs as a biolatex for paper coatings to allow ease of manufacturing and application. However, glycerol, being a triol with two primary alcohol groups, strongly interferes with the oxidation via TEMPO. Attempting to oxidize starch with glycerol present will result in a much lower yield of carboxylated starch, and any subsequent amide coupling reactions with DNA will fail.

Glycerol can be removed via purification in a dimethyl sulfoxide (DMSO) solution. ENPs can be soaked in 10% w/w DMSO aqueous solution in 4°C overnight. Precipitation in cold methanol will remove glycerol and purify the resulting ENP for chemical modification.

### 4.2.3 C6-Selectivity

The selectivity for primary hydroxyl groups via TEMPO was tested by attempting to oxidize dextran in place of starch. Dextran, another polysaccharide, differs from starch such that the glucose units are linked via α-1,6 glycosidic bonds rather than α-1.4 bonds. This occupies the primary hydroxyl group on the 6′ carbon of the glucose unit while exposing the secondary hydroxyl group on the 4′ carbon. The oxidation reaction proceeded as previously mentioned. However, the addition of sodium hypochlorite did not lower the pH of the solution, indication that acidic components were not formed, and the oxidation reaction did not proceed. This confirms the selectivity for primary hydroxyl groups for TEMPO, i.e. that TEMPO favours the 6′ carbon in glucose, and the unavailability of the hydroxyl group in dextran means that oxidation via TEMPO cannot proceed.

### 4.2.4 pH Control

The control of the solution pH is essential for successful oxidation. The optimal pH for TEMPO is between 8.5 and 11.5, with a significant drop in the rate of reaction outside this range.[99] Below

pH 8.5, the relative abundance of protons in solution will deter oxidation, and the reaction will not proceed. At pH 11.5, a more serious problem occurs in that the degradation of starch is significant, and the ENPs compact and form a deep brown viscous gel-like structure upon precipitation in ethanol (Figure 4.2). This gel-like structure is irreversible, and does not revert back to its old white powdery characteristics when lyophilized, re-dispersed in water, when pH is lowered towards neutral, or solution temperature is raised.

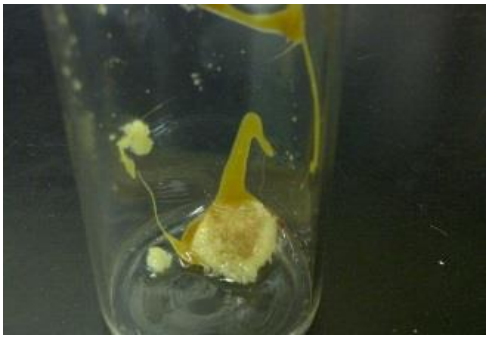

**Figure 4.3**: Irreversibly degraded starch nanoparticles.

## 4.3 EDC-NHS Coupling

The coupling of an amine with a carboxyl group to form an amide can be done through many methods. One such method is the use of a carbodiimide as a coupling agent, with 1-ethyl-3-(3-dimethylaminopropyl)carbodiimide (EDC, available as a hydrochloride salt) being a popular example due to its water solubility and ease of use. A second agent, N-hydroxysuccinimide (NHS), is also introduced to stabilize the reaction. The resulting amide bond is formed with EDC consumed and NHS regenerated.

### 4.3.1 Theory

EDC is used to activate carboxyl groups and prime it for further reaction. In low pH, the carbodiimide will be able to react with a dissociated carboxyl group. This intermediate is unstable and labile in aqueous solutions, which necessitates the immediate reaction with an anime or alcohol to form an amide or ester, respectively.[100] Alternatively, NHS can be introduced to form an ester, whereas the resulting esterification produces a more stable intermediate, but the succinimide remains a good leaving group.[101] Primary amines can then be used to displace the succinimide to produce a stable amide. For a carboxylated starch nanoparticle and an amine-labeled DNA strand, this can produce a covalent linkage between starch and DNA via an amide bond produced through EDC/NHS coupling (Figure 4.3).

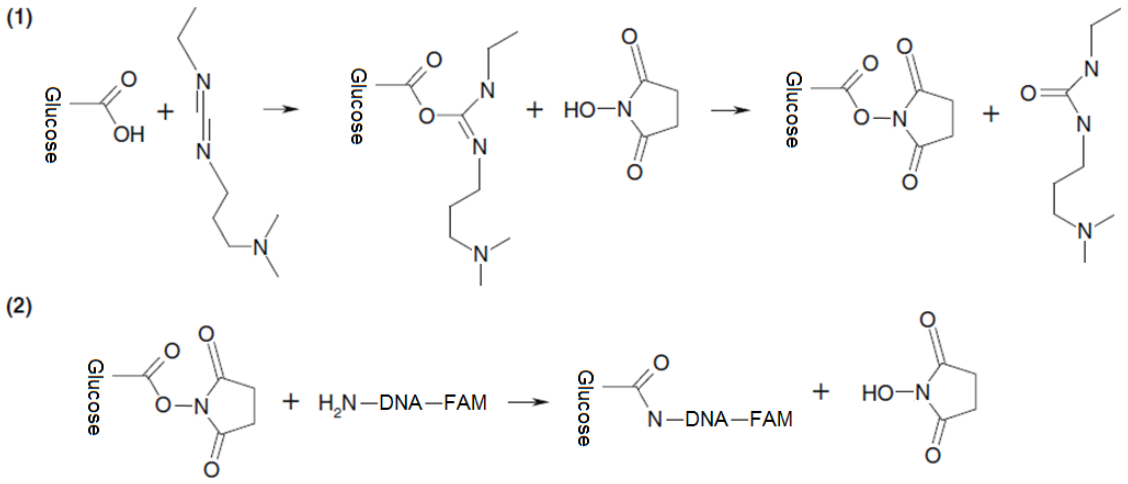


**Figure 4.4**: Proposed mechanism for linking DNA onto starch through an EDC/NHS coupling reaction. (1) Initial activation by EDC/stabilization by NHS (2) Final amide formation via amine-labeled DNA.

A typical conjugation protocol would proceed as such: ENPs were prepared in 1% or 5% w/w in Milli-Q water. AS1411 DNA was prepared in 100 mM HEPES buffer at 50 µM concentration. 400 mM EDC and 100 mM NHS was prepared each in 50 mM MES and 50 mM NaCl, with both solutions made fresh. The ENPs were primed by the addition of EDC and NHS for 5-10 minutes. 50 µL of AS1411 was added afterwards, briefly vortexed for good mixing, then allowed to incubate in ambient conditions away from light for 1 hour. The ENPs were purified from unreacted components via ethanol precipitation and the mixture centrifuged at 15000 RPM for 30 minutes, then resuspended in Milli-Q water at the original concentration.

### 4.3.2 Issues

To test for successful binding, polyacrylamide gel electrophoresis (PAGE) was run with the resuspended samples. As 15% polyacrylamide produces a gel with comparatively smaller pore sizes, it is expected that the ENPs would not be able to migrate through the gel, but rather remain in the loading wells at the top of the gel. The smaller FAM-labeled AS1411 DNA, however, would be able to migrate into the gel similar to the DNA precipitation procedure, unless a successful conjugation took place. As AS1411 is an ssDNA, ethidium bromide staining will necessarily fail; ethidium bromide can only intercalate dsDNA to produce a fluorescence signal.[102] However, as AS1411 is already labeled with FAM, additional labeling with ethidium

bromide would be unnecessary. The location of the fluorescence would determine whether or not successful coupling took place; as an excess of DNA was introduced, fluorescence in the gel would be inevitable, but fluorescence in the loading wells as well would be indicative of a successful conjugation. If the starch nanoparticles are able to migrate through the gel along with the unconjugated free DNA, then the progress would be hindered by the much larger starch size, and a separate band or a large-area smear would be expected to be seen within the channel.

To test the effectiveness of PAGE, the supernatant of precipitated ENPs were run through PAGE first. Ethanol can cause DNA to precipitate out by aggregation.[81] The aggregation is typically caused by ethanol being a much less polar solvent than water; this causes inter-helical interactions to increase and aggregate DNA together. These aggregates typically can be re-dispersed through the removal of ethanol and re-introduction of water as a solvent. During PAGE, TBE buffer is introduced as part of an aqueous solution. However, the DNA strands do not migrate as a flat band as expected for free DNA; instead they migrate out as a misshapen band (Figure 4.4), which suggests that there is additional interference by ethanol during PAGE. This smear is present even when no binding was expected, such as for samples with no EDC or NHS present. The gel was performed with NCC as a control to rule out ENPs as the cause for interference.

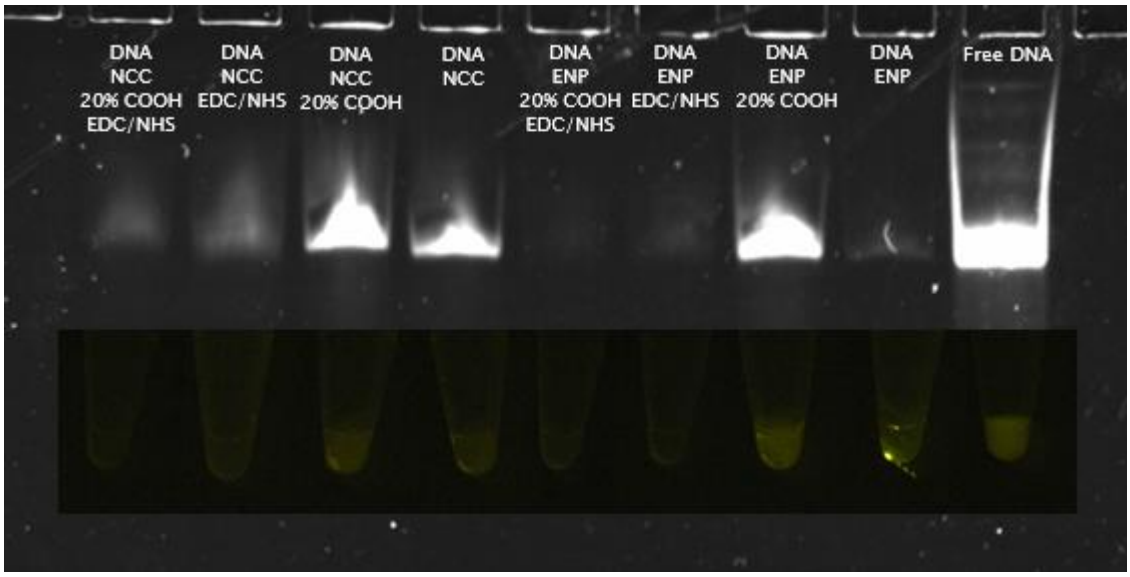


**Figure 4.5**: Fluorescence photograph of PAGE run on DNA-starch conjugates after ethanol precipitation. Significant loss of quality of bands are observed for all samples which have ethanol precipitation. Inset: Photographs of samples after ethanol precipitation and centrifugation.

The gel in Figure 4.4 attempted to verify the efficacy of EDC/NHS coupling by having the conjugation performed on both oxidized and unoxidized ENPs, as well as both oxidized and unoxidized NCCs as a control. Unfortunately, none of them showed any appreciable fluorescence in the loading wells; those with EDC and NHS introduced also showed a remarkable lowered overall fluorescence in the band, suggesting something else may be interfering.

### 4.3.3 Potential EDC-Mediated Fluorescence Quenching

The potential fluorescence quenching via EDC was further explored. The previous experiment was repeated, except the ethanol precipitation to purify the samples was not performed; this step was deemed unnecessary as unconjugated DNA can still be separated by PAGE. The resulting gel confirmed that ethanol is indeed responsible for the unusual DNA band shape; the presence of EDC and NHS continued to quench the fluorescence of DNA (Figure 4.5). This quenching is problematic due to the inability to identify whether or not DNA was successfully conjugated to starch found in the loading wells of the PAGE gel.

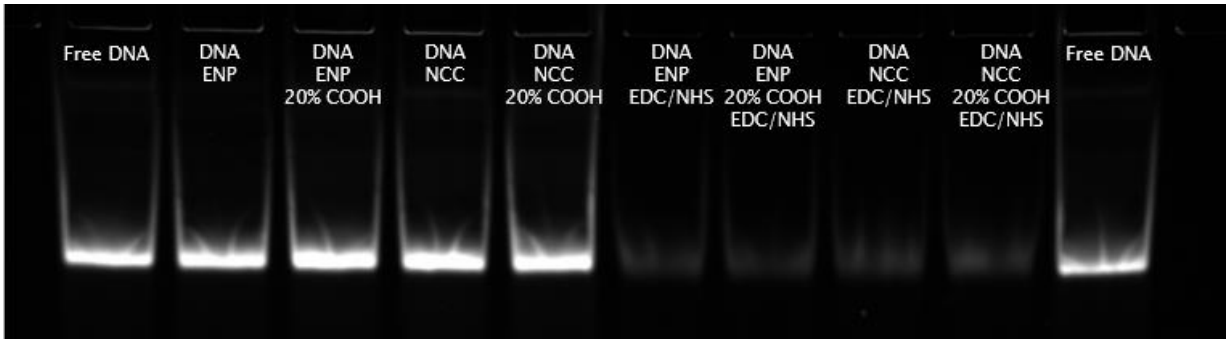


**Figure 4.6**: Fluorescence image of PAGE run on DNA-starch conjugates before ethanol precipitation.

Next, the dependence of quenching on the concentration of EDC was tested. The concentration of EDC used was reduced by a quarter and by one-sixteenth (to 100 mM and 25 mM), while all other factors remained constant. Both FAM-labeled DNA and Cy3-labeled DNA were used to test the dependence of quenching by fluorophore. Regardless of whether or not the ENPs used were oxidized, or even whether or not they were present at all, the fluorescence was partially restored with the reduction of EDC used (Figure 4.6). The quenching mechanism has not been explored in-depth, although its existence is surprising given that the EDC-NHS coupling mechanism is quite well-known and widely used.

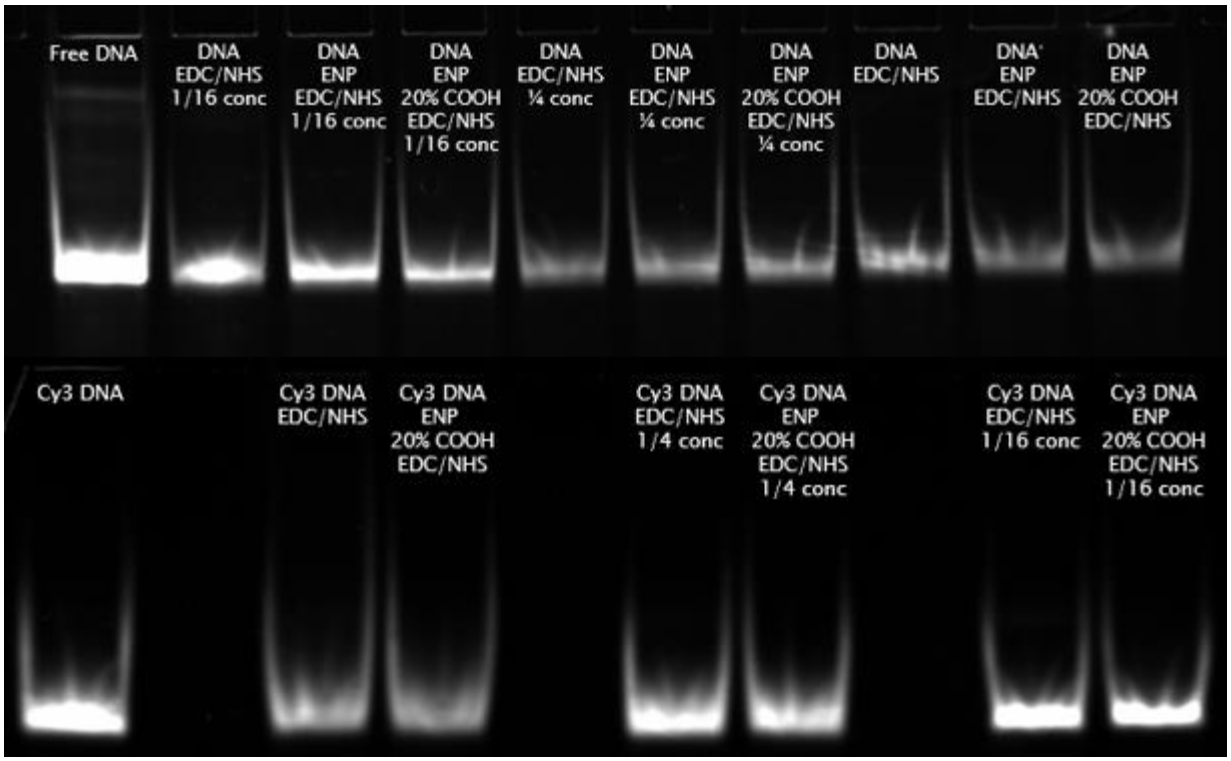


**Figure 4.7**: Concentration dependent quenching of fluorescence of FAM (top) and Cy3 (bottom) by EDC

It should be noted that fluorescein derivatives such as FAM have an optimal pH operation range of 7-9, and typically have reduced fluorescence activity in acidic pH.[103,104] This activity can typically be recovered by reintroducing the fluorophore to higher basic pH levels.[105] During the incubation period, EDC and NHS are introduced in an MES/NaCl buffer at pH 6. This pH is low enough to potentially reduce fluorescence; however subsequent fluorescence readings are performed after resuspension in HEPES buffer (pH 7.6) for plate reading, or in TBE buffer (pH 8.3) for PAGE. These slightly basic conditions should be enough to restore fluorescence activity, and have been shown to do so for free FAM-DNA samples.

To further investigate the generalizability of the quenching, the FAM-labeled DNA was replaced with a FITC-cadaverine fluorophore. This construct removed the DNA portion of the ligand, leaving only the fluorophore with a short diamine ligand for coupling via EDC-NHS conjugation. This would also serve to increase the signal output, as the G-rich sequence of the AS1411 aptamer may itself quench the FAM fluorescence and lower the signal output. By repeating the same PAGE protocol, a boost in signal would be expected from using FITC-cadaverine instead of AS1411 to verify the success of the conjugation reaction (Figure 4.7).

Although FITC-cadaverine is not a polyanion like DNA, it is still able to migrate through the acrylamide gel, albeit with a larger diffusion artifact. A slight loading error was made with the loading of the FITC/ENP 20% COOH with 1/16 EDC dilution sample, producing a signal diluted by half. This directly affected the fluorescence of the signal, but the still illustrated the direct effect of fluorescence quenching by EDC.

The increase in signal intensity, however, helps confirm that the conjugation is still successful despite the reduced ability to identify the nanoparticles. Although difficult to visualize in the ENP samples, the positive control samples with NCC have loading wells showing a clear fluorescence signal (Figure 4.7 circled in red), demonstrating that successful conjugation has taken place.

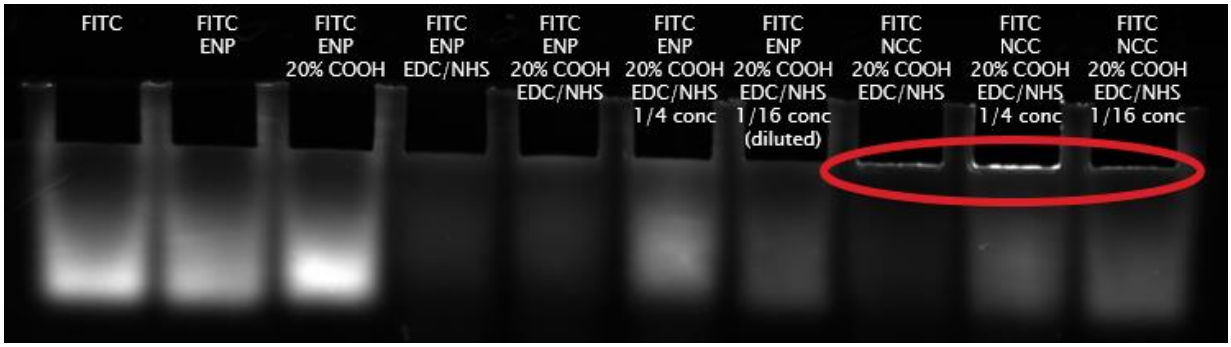


**Figure 4.8**: Fluorescence image of PAGE run on FITC-cadaverine-starch/NCC, with successful coupling. The circle shows dye successfully conjugated to NCCs

To quantify the quenching of fluorescence by EDC, fluorescence readings were taken of the samples. As NCCs can be centrifuged without ethanol precipitation, readings were performed on NCCs for easier handling and to avoid possible artifacts brought about by ethanol precipitation. The protocol was repeated up to the ethanol precipitation stage, where NCC samples were simply centrifuged without the addition of ethanol. The supernatant was separated from the resultant NCC pellets, and the pellets resuspended in 100 mM HEPES buffer. A pellet was "assumed" for free dye; although accuracy is lost, the magnitude of difference in signal intensities makes absolute accuracy unnecessary. Fluorescence readings of the two were performed by taking 5 µL of the sample and adding to 95 µL of 100 mM HEPES buffer and averaged over 4 readings (Figure 4.8). There was a progressively smaller difference between supernatant and pellet readings for increasingly diluted EDC concentrations, but also a higher

overall reading of the pellet and supernatant values summed together. This would make sense as a lower amount of EDC would lead to less binding of FITC-cadaverine to the NCCs, but also to less quenching of the FITC dye in general.

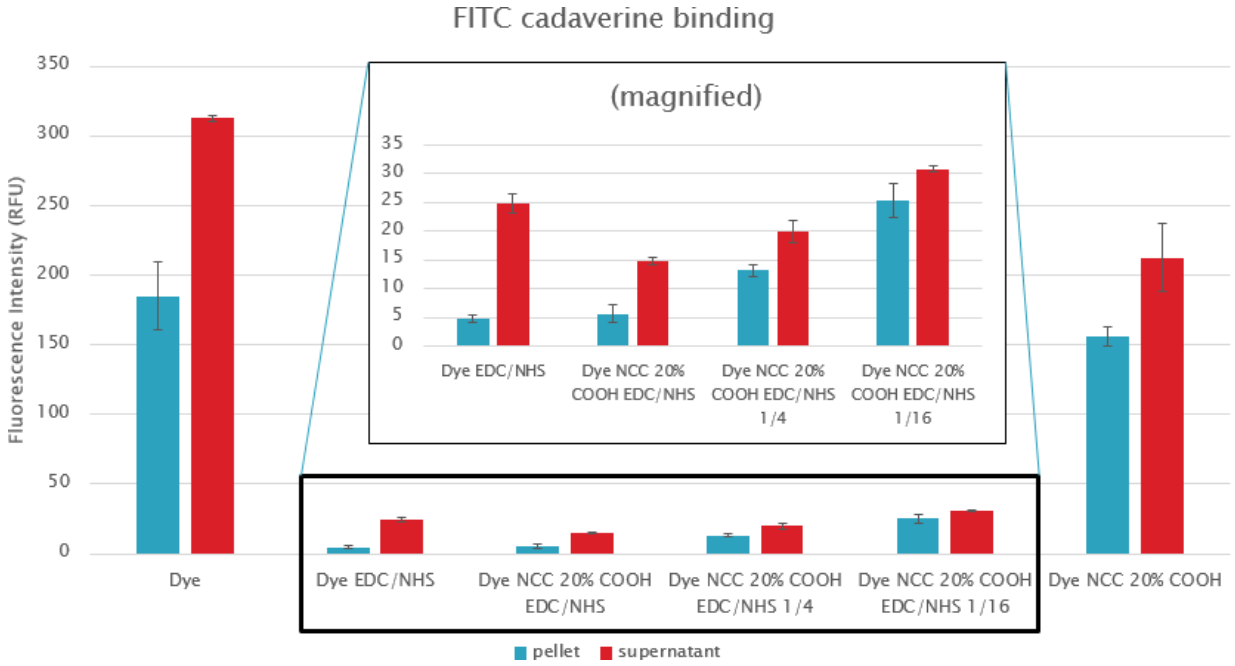


**Figure 4.9**: Fluorescence readings of conjugated NCCs with varying concentrations of EDC.

## 4.4 Introduction of Starch-DNA conjugates to cells

The starch nanoparticles could be used for delivery of therapeutic substances into cells. Starch, being a food-grade substance, would be easily biocompatible compared to previously explored nanoparticle formulations. A lot of the shortfalls found in the creation of other similar targeted delivery vehicles can be avoided using starch, such as having a much simpler nanoparticle structure, having all formulations created in an aqueous environment, and not requiring potentially toxic or carcinogenic substances that are incorporated into the nanoparticle. Free AS1411, although having potential therapeutic benefits of its own, will be used solely for its targeting abilities and its high affinity for the nucleolin protein.

### 4.4.1 HeLa properties

The HeLa cell line is a widely popular line used as a model cancer cell line. It is the first immortal cell line harvested from a cancer patient, and the name HeLa was derived from the patient's name Henrietta Lacks.[106] The cells were harvested from her cervix as an adenocarcinoma. HeLa cells are hardy and easily cultivatable, replicating every 24 hours, leading to their widespread

use in the scientific community. Their hardiness has led to their lines proliferating as contaminants of other lines, given their ability to grow in a wide range of conditions.[107]

HeLa cells are known to express nucleolin, which is essential for cell proliferation and stress response.[108] This makes it an excellent model for targeting with AS1411, to see if HeLa cells can uptake the AS1411-modified ENPs.

### 4.4.2 Cell Uptake and Endocytosis

For the formulation of ENPs for cell uptake, there was some concern that the EDC-mediated quenching of fluorescence would make it harder to detect the FAM fluorescence from the AS1411. The protocol for conjugating AS1411 onto starch was changed so that 0.5% w/v ENPs was used instead; this allowed a higher concentration of AS1411-conjugated ENPs to enter cells, and potentially raise the fluorescence signal that would be received.

The HeLa cell line was cultivated using DMEM/F-12 1:1 cell growth medium, formulated with 10% fetal bovine serum and 1% penicillin-streptomycin antibiotic, then seeded into a standard 96-well plate before being introduced to AS1411-conjugated ENPs. The final concentration of introduced ENPs was at 0.05% w/v. Cells with ENPs were incubated at 37°C with 95% relative humidity and 5% $CO_2$. The HeLa nuclei were stained with Hoechst 33342, then the wells were washed with phosphate buffered saline. Images were taken using a fluorescence microscope with camera attached (Figure 4.9). Composite images were created using a brightfield view, DAPI filter set view, and FITC filter set view, and superimposed. Images from only the FITC filter set was also taken for direct comparison for binding efficiency. It can be seen that although all 3 samples have some fluorescence binding, only the cells given oxidized ENPs with AS1411 show significant fluorescence signal from the AS1411. Free AS1411, although having known activity to nucleolin found on HeLa cells, did not bind particularly strongly to the cells. Unoxidized ENPs with AS1411 also did not have a particularly strong signal, due to free AS1411 being washed away during the purification steps. It should be noted that although the fluorescence signals from the AS1411 conjugated onto the oxidized ENPs shows fluorescence, the signal is still comparatively weak, requiring longer exposure times to pick up, and also is not fully localized with cells, suggesting particle aggregation and incomplete uptake into cells.

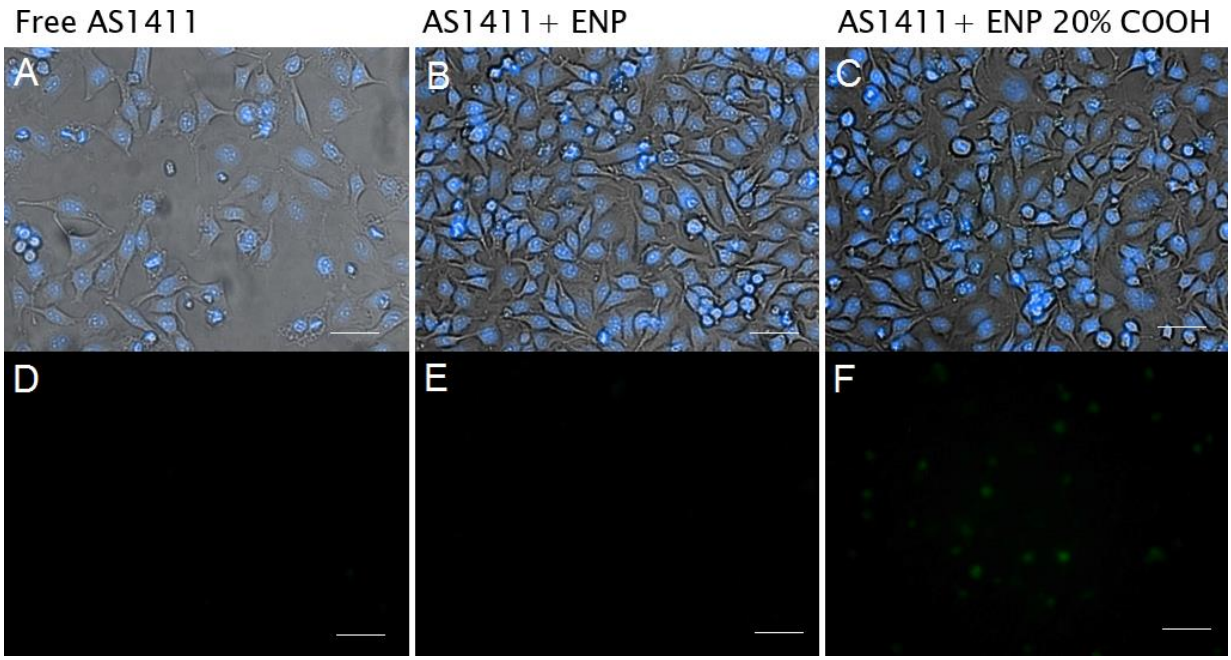


**Figure 4.10**: HeLa cells incubated with free AS1411, conjugated to native and oxidized ENPs.The cells had a slightly higher confluency than anticipated. A-C: Composites of brightfield, Hoechst 33342 and FAM together, D-F: Images of only the FAM channel displayed.

## 4.5 Materials and Methods

Starch nanoparticles (bulk production ENPs) were graciously provided by EcoSynthetix Inc. (Hamilton, Ontario). NCCs were produced as described above from Whatman filter paper (Madstone, England). Dextrin (from corn, commercial grade, Type II) and dextran (from *Leuconostoc* spp.) were purchased from Sigma-Aldrich (St. Louis, Missouri). HEPES, MES, and NaCl salts, DMSO, and sodium hydroxide were purchased from Mandel Scientific (Guelph, Ontario). FAM/Cy3 and amine dual-labeled DNA sequences AS1411 was purchased from Integrated DNA Technologies (Coralville, Iowa). EDC and NHS were purchased from Sigma-Aldrich (St. Louis, Missouri). Ammonium persulfate, TEMED, TBE buffer, and acrylamide/bis-acrylamide (40% solution, 29:1) were purchased from Bio Basic Canada (Markham, Ontario). Dulbecco's Modified Eagle Medium/F-12 Cell Culture Medium 1:1 and phosphate buffered saline were purchased from Arch Chemicals (Mississauga, Ontario). Fetal bovine serum and Hoechst 33342 were purchased from Thermo Scientific (Waltham, Massachusetts). Penicillin-Streptomycin was purchased from Corning Life Sciences (Corning, New York). Sodium hypochlorite was purchased from Ricca Chemical Company (Arlington, Texas). HeLa cells

(CCL-2™) were obtained from ATCC (Manassas, Virginia) through the gracious help of the labs of Dr. Shirley Tang and Dr. Michael Palmer (Waterloo, Ontario).

### 4.5.1 Oxidation of Starch Nanoparticles

The oxidation of ENPs typically follows the protocol as described by Kato *et al.*[98] A 100 mL dispersion of 5% w/w ENPs is prepared by adding 5 g of ENPs into 100 mL Milli-Q water while stirring at 80°C, and allowed to disperse for 30 min. TEMPO and NaBr are added at 0.01 and 0.2 molar ratio per anhydroglucose unit, respectively, into a second vessel containing 100 mL Milli-Q water. Assuming availability of all 6′ carbons of anhydroglucose units along ENPs gives 30.8 mmol of oxidation sites, so 48.2 mg (308 µmol) of TEMPO and 635 mg (6.17 mmol) of NaBr are dissolved under stirring. The starch solution is brought to under 5°C using an ice-water frigorific bath, and the two solutions are mixed together. The pH is monitored and raised to just above 10 by the slow addition of 0.5 M NaOH. Care is taken to ensure pH is not raised above 10.1. Oxidation proceeds through the addition of 5% w/w sodium hypochlorite solution according to the desired incomplete oxidation amount. For 20% oxidation, 12.3 mL of sodium hypochlorite solution are added slowly. Successful oxidation is monitored by a corresponding pH drop. As sodium hypochlorite naturally has a fairly high pH of above 10, the slow addition allows the pH to drop without first experiencing a spike of basicity. A pH between 10 and 10.1 is maintained through the continuous slow addition of 0.5 M NaOH. The protocol proposed here differs from literature such that a pH of 10.75 is avoided to minimize depolymerisation;[8] the reaction will still proceed albeit at a slightly slower rate.

The reaction is allowed to proceed until pH stabilizes with no change over 10 minutes. The reaction is then quenched by the addition of a triple volume of ethanol; the exact volume varies depending on how much NaOH was added, but approximately 750 mL of ethanol would be required. The precipitated starch would take on a flocculated appearance, and appear white or off-white in colour. The precipitants can be collected via centrifugation at 3000 RCF for 10 minutes. The supernatant was discarded, and the precipitants resuspended and re-precipitated for a total of 3 washes. Measurements of pH were performed to confirm neutrality was reached, before the resultant ENP precipitants were lyophilized to remove remaining solvents.

This protocol was also used for the oxidation of NCCs; it is expected the kinetics for the reaction may be different due to the availability of less surface area due to the crystalline nature of NCCs, such that not all 6′ carbons are accessible for oxidation.

### 4.5.2 Conjugation of Amine-Labeled DNA onto Oxidized Starch

The conjugation reaction typically proceeds with the activation of the carboxyl by EDC, stabilization by NHS, and finally amide formation by amine-labeled DNA. Solutions of ENPs, amine-labeled AS1411 with FAM, EDC, and NHS were prepared before mixing. ENPs were prepared in 1% w/w in Milli-Q water. 10 μM AS1411 DNA was prepared in 100 mM HEPES buffer. 400 mM EDC was prepared by dissolving 38.2 g of EDC into 500 μL of 50 mM MES and 50 mM NaCl. 100 mM NHS was prepared by dissolving 11.5 g of NHS into 1 mL in 50 mM MES and 50 mM NaCl. Due to EDC's instability in water, EDC solutions must be prepared fresh each time. Solutions of NHS are also unstable, but exhibit a much longer half-life than EDC; as a precaution NHS solutions should also be prepared fresh. 50 μL of ENP solution was primed with 200 μL of EDC and 200 μL of NHS for 5-10 minutes. 50 μL of AS1411 was added afterwards, briefly vortexed for good mixing, then allowed to incubate in ambient conditions in the dark for 1 hour. ENPs were purified by the addition of 1 mL of ethanol for ethanol precipitation, and centrifuged at 21000 RCF. Occasionally smaller volumes were used, and reagents were scaled accordingly. For example, if only 20 μL of sample was required (*e.g.* for PAGE analysis), then 2 μL for ENPs and AS1411, 8 μL for EDC and NHS, and 40 μL for ethanol can be used for successful conjugation of a small volume. Dynamic light scattering and ζ-potential measurements were performed on a Malvern Zetasizer Nano ZS90. Averages of 3 runs were made, each run consisting of 10 measurements for 1 minute each. Concentrations of 0.05% w/v ENPs were used.

This protocol was followed both when oxidized ENPs were replaced with oxidized NCCs, and when amine-labeled AS1411 was replaced with FITC-cadaverine.

### 4.5.3 Polyacrylamide Gel Electrophoresis

Polyacrylamide gel electrophoresis was performed on a 15% acrylamide/bis-acrylamide gel. A 250 mL stock solution of 15% acrylamide/bis-acrylamide was created by adding 156.25 mL of Milli-Q water to 93.75 mL of 40% acrylamide/bis-acrylamide. For casting acrylamide gel, 22 mL of the 15% solution was added to a volumetric flask along with 50 mL of 10% w/w aqueous ammonium persulfate as initiator and 20 mL of TEMED as catalyst. Gel casting equipment was obtained from C.B.S. Scientific (Del Mar, California). Gels were cast for 90 minutes to allow the polymerization to proceed and form wells for loading samples. Wells were rinsed with TBE buffer before the addition of samples. Electrophoresis of ENPs were performed by loading 20

µL of the samples directly into the wells with 20 µL of 30% w/w of glycerol. The gel electrophoresis was performed at 500 V and 250 mA for 30 minutes using a 2060P power supply from Thermo Scientific (Waltham, Massachusetts). Fluorescence images of the stained gel was obtained using a Gel-Doc Universal Hood III with fluorescein filter from Bio-Rad Life Sciences (Mississauga, Ontario).

### 4.5.4 Introduction of Starch Nanoparticles to HeLa Cells

HeLa cells were cultured in a biosafety level 2 facility found in the laboratory of Dr. Michael Palmer, with the assistance of the laboratory of Dr. Shirley Tang. Proper aseptic techniques were adhered to for the duration of the culturing period. Cells were cultured using DMEM/F-12 1:1 media with 10% v/v fetal bovine serum and 1% v/v penicillin-streptomycin. Cells were seeded into a standard 96-well plate with 70% confluency. 10 µL of 0.5% ENPs or 1 µM free AS1411 was introduced to the cells and allowed to incubate for 2 hours in 37°C with 5% $CO_2$ and 95% humidity. Afterwards, cells were stained with 1 µL of 10 mg/mL of Hoechst 33342 for 2 minutes, then rinsed with 100 µL phosphate buffered saline. Cells were imaged while immersed in 100 µL phosphate buffered saline using a Nikon Eclipse T*i* inverted microscope system with Intensilight fluorescence. Brightfield images were taken with 50 ms exposure time, DAPI filter (ex. 360 nm, em. 460 nm) fluorescence images were taken with 200 ms exposure time for imaging Hoechst 33342, and FITC filter (ex. 480 nm, em. 535 nm) fluorescence images were taken with 5 seconds exposure for imaging FAM on AS1411; this unusually long exposure time was required to account for the EDC-mediated quenching of the fluorophore which hinders detection of the ENP-DNA nanoparticle.

## 4.6 Conclusion and Future Work

It has been demonstrated that starch nanoparticles functionalized with AS1411 aptamer can successfully bind to HeLa cancer cells. However, cellular uptake has not been confirmed, and the fluorescence image indicates a larger particle than anticipated, suggesting aggregation may have taken place. The use of techniques such as confocal microscopy can further determine cellular uptake, as the insides of the cell can be imaged as well. In addition, the coupling protocol can be further optimized to see if the fluorescence signal quenching can be mitigated, such that a visual confirmation of successful binding can be seen. Alternatively, techniques such as infrared spectroscopy or nuclear magnetic resonance may also potentially confirm these bonds.

Future work can include the loading of antineoplastic drugs into the nanoparticles, and measuring its efficacy in causing cell death. Techniques such as MTT assay or live-dead staining can further assist in determining the efficacy of the starch nanoparticles and its suitability as a drug delivery vehicle. Once conditions can be optimized, additional options for *in vivo* work may be explored as part of the process of developing a fully-functional drug delivery vehicle for clinical use.

## 5.0 CONCLUSION

Starch-based nanoparticles have shown tremendous promise in becoming a substitute for petroleum-based products as a renewable biopolymer substitute. Given its abundance and low cost, exploring its potential in replacing non-renewable resources is imperative. Expanding its use into less traditional niches is a logical next step for increasing the utility of this material.

Starch nanoparticles have been found to co-precipitate DNA with high efficiency with ethanol precipitation. This co-precipitation is applicable to a wide range of DNA, including a range of lengths and sequences. The co-precipitation can also take place in a wide range of pH values, salt concentrations, and is applicable to both single-stranded and double-stranded DNA. The driving force behind this adsorption has not been determined; although hydrogen bonding was suspected at first, its applicability in both high and low pH values suggests other forces may be at play.

The covalent attachment of DNA onto starch nanoparticles has shown moderate success. Originally, difficulties were encountered with the unexpected quenching of fluorescence by the coupling agent used. This made it difficult to confirm if proper covalent attachment has actually taken place. However, by using the native fluorophore which does not exhibit systemic quenching, the fluorescence signal can be boosted sufficiently such that it can be shown attachment does take place properly. This is confirmed with the introduction of DNA-functionalized starch nanoparticles to HeLa cells.

### 5.1 Future Work

Although the starch-DNA interactions have been characterized to show good applicability, further analysis can be performed. Using starch as a co-precipitant can be measured and compared quantitatively with other existing methods; while starch nanoparticles have been shown to be excellent co-precipitants in a set of conditions defined herein, a comparison can be made to see if starch can be used as a co-precipitant in traditional ethanol precipitation protocols, adding it to the ranks of linear polyacrylamide and glycogen as a lower-cost alternative. Conversely, linear polyacrylamide and glycogen can be compared by using it as a co-precipitant in replacing starch while following the protocols defined in this thesis report. A side-by-side comparison may shed further insight as to which co-precipitant is more effective in ethanol precipitation.

In addition, the driving force behind the co-precipitation of starch and DNA has not been elucidated yet. While hydrogen bonding was first suspected, it has since been ruled out as a possibility due to the pH insensitivity of the technique. Additional research may determine the underlying cause for this, and perhaps improve the efficiency of this technique even more.

Starch nanoparticles have been successfully introduced to HeLa cells with successful binding suggested. However, its distribution is less than ideal, suggesting there may be aggregation in the nanoparticles that may hinder complete endocytosis into the cells. Further work may be performed that may investigate this phenomenon, and determine if this potential aggregation is reversible or not. In addition, to be used as a drug delivery vehicle, the nanoparticle should be loaded with antineoplastic agents, and delivered into cells. Its efficacy in killing cancer cells should be measured against the delivery of free drugs in solution, to see if a sustained dose can be maintained. Once these parameters have been optimized, research may continue into using the starch nanoparticles for *in vivo* application towards a therapeutic delivery vehicle.

## LETTERS OF COPYRIGHT PERMISSION

### ELSEVIER LICENSE
### TERMS AND CONDITIONS

Jul 03, 2013

This is a License Agreement between Alexander Ip ("You") and Elsevier ("Elsevier") provided by Copyright Clearance Center ("CCC"). The license consists of your order details, the terms and conditions provided by Elsevier, and the payment terms and conditions.

**All payments must be made in full to CCC. For payment instructions, please see information listed at the bottom of this form.**

| | |
|---|---|
| Supplier | Elsevier Limited<br>The Boulevard,Langford Lane<br>Kidlington,Oxford,OX5 1GB,UK |
| Registered Company Number | 1982084 |
| Customer name | Alexander Ip |
| Customer address | 55 Havendale Road<br>Scarborough, ON M1S1E3 |
| License number | 3173311178297 |
| License date | Jun 20, 2013 |
| Licensed content publisher | Elsevier |
| Licensed content publication | Current Opinion in Plant Biology |
| Licensed content title | Improving starch for food and industrial applications |
| Licensed content author | Steve Jobling |
| Licensed content date | April 2004 |
| Licensed content volume number | 7 |
| Licensed content issue number | 2 |
| Number of pages | 9 |
| Start Page | 210 |
| End Page | 218 |
| Type of Use | reuse in a thesis/dissertation |

| | |
|---|---|
| Portion | figures/tables/illustrations |
| Number of figures/tables/illustrations | 1 |
| Format | both print and electronic |
| Are you the author of this Elsevier article? | No |
| Will you be translating? | No |
| Order reference number | |
| Title of your thesis/dissertation | Interactions between DNA and starch nanoparticles: adsorption and covalent attachment |
| Expected completion date | Aug 2013 |
| Estimated size (number of pages) | 80 |
| Elsevier VAT number | GB 494 6272 12 |
| Permissions price | 0.00 USD |
| VAT/Local Sales Tax | 0.00 USD / 0.00 GBP |
| Total | 0.00 USD |

---

## JOHN WILEY AND SONS LICENSE TERMS AND CONDITIONS

Jul 03, 2013

---

---

This is a License Agreement between Alexander Ip ("You") and John Wiley and Sons ("John Wiley and Sons") provided by Copyright Clearance Center ("CCC"). The license consists of your order details, the terms and conditions provided by John Wiley and Sons, and the payment terms and conditions.

**All payments must be made in full to CCC. For payment instructions, please see information listed at the bottom of this form.**

| | |
|---|---|
| License Number | 3177231444483 |
| License date | Jun 27, 2013 |
| Licensed content publisher | John Wiley and Sons |

| | |
|---|---|
| Licensed content publication | Starch |
| Licensed content title | Starch Modification Using Reactive Extrusion |
| Licensed copyright line | Copyright © 2006 WILEY-VCH Verlag GmbH & Co. KGaA, Weinheim |
| Licensed content author | Fengwei Xie,Long Yu,Hongshen Liu,Ling Chen |
| Licensed content date | Mar 22, 2006 |
| Start page | 131 |
| End page | 139 |
| Type of use | Dissertation/Thesis |
| Requestor type | University/Academic |
| Format | Print and electronic |
| Portion | Figure/table |
| Number of figures/tables | 1 |
| Original Wiley figure/table number(s) | Figure 1 |
| Will you be translating? | No |
| Total | 0.00 USD |

---

**SPRINGER LICENSE**
**TERMS AND CONDITIONS**

Jul 03, 2013

---

---

This is a License Agreement between Alexander Ip ("You") and Springer ("Springer") provided by Copyright Clearance Center ("CCC"). The license consists of your order details, the terms and conditions provided by Springer, and the payment terms and conditions.

**All payments must be made in full to CCC. For payment instructions, please see information listed at the bottom of this form.**

| | |
|---|---|
| License Number | 3177231245206 |
| License date | Jun 27, 2013 |
| Licensed content publisher | Springer |
| Licensed content publication | Journal of Materials Science: Materials in Medicine |
| Licensed content title | Dynamics of controlled release of heparin from swellable crosslinked starch microspheres |

| | |
|---|---|
| Licensed content author | A. K. Bajpai |
| Licensed content date | Jan 1, 2007 |
| Volume number | 18 |
| Issue number | 8 |
| Type of Use | Thesis/Dissertation |
| Portion | Figures |
| Author of this Springer article | No |
| Order reference number | |
| Title of your thesis / dissertation | Interactions between DNA and starch nanoparticles: adsorption and covalent attachment |
| Expected completion date | Aug 2013 |
| Estimated size(pages) | 80 |
| Total | 0.00 USD |

---

**ELSEVIER LICENSE**
**TERMS AND CONDITIONS**

Jul 03, 2013

---

---

This is a License Agreement between Alexander Ip ("You") and Elsevier ("Elsevier") provided by Copyright Clearance Center ("CCC"). The license consists of your order details, the terms and conditions provided by Elsevier, and the payment terms and conditions.

**All payments must be made in full to CCC. For payment instructions, please see information listed at the bottom of this form.**

| | |
|---|---|
| Supplier | Elsevier Limited<br>The Boulevard,Langford Lane<br>Kidlington,Oxford,OX5 1GB,UK |
| Registered Company Number | 1982084 |
| Customer name | Alexander Ip |
| Customer address | 55 Havendale Road<br>Scarborough, ON M1S1E3 |
| License number | 3176080458233 |
| License date | Jun 25, 2013 |

| | |
|---|---|
| Licensed content publisher | Elsevier |
| Licensed content publication | Carbohydrate Polymers |
| Licensed content title | Oxidation process of water-soluble starch in TEMPO-mediated system |
| Licensed content author | Y Kato,R Matsuo,A Isogai |
| Licensed content date | 1 January 2003 |
| Licensed content volume number | 51 |
| Licensed content issue number | 1 |
| Number of pages | 7 |
| Start Page | 69 |
| End Page | 75 |
| Type of Use | reuse in a thesis/dissertation |
| Intended publisher of new work | other |
| Portion | figures/tables/illustrations |
| Number of figures/tables/illustrations | 1 |
| Format | both print and electronic |
| Are you the author of this Elsevier article? | No |
| Will you be translating? | No |
| Order reference number | |
| Title of your thesis/dissertation | Interactions between DNA and starch nanoparticles: adsorption and covalent attachment |
| Expected completion date | Aug 2013 |
| Estimated size (number of pages) | 80 |
| Elsevier VAT number | GB 494 6272 12 |
| Permissions price | 0.00 USD |
| VAT/Local Sales Tax | 0.00 USD / 0.00 GBP |
| Total | 0.00 USD |

## REFERENCES


1. Siddique, R., Khatib, J. & Kaur, I. Use of recycled plastic in concrete: a review. *Waste management (New York, N.Y.)* **28**, 1835–52 (2008).

2. Mohanty, A. K., Misra, M. & Drzal, L. T. Sustainable Bio-Composites from Renewable Resources : Opportunities and Challenges in the Green Materials World. **10**, 19–26 (2002).

3. Ellis, R. P. *et al.* Starch production and industrial use. *Journal of the Science of Food and Agriculture* **77**, 289–311 (1998).

4. Jayasena, S. D. Aptamers: an emerging class of molecules that rival antibodies in diagnostics. *Clinical chemistry* **45**, 1628–50 (1999).

5. Tester, R. F., Karkalas, J. & Qi, X. Starch—composition, fine structure and architecture. *Journal of Cereal Science* **39**, 151–165 (2004).

6. Ayoub, a. S. & Rizvi, S. S. H. An Overview on the Technology of Cross-Linking of Starch for Nonfood Applications. *Journal of Plastic Film and Sheeting* **25**, 25–45 (2009).

7. Singh, J. Studies on the morphological and rheological properties of granular cold water soluble corn and potato starches. *Food Hydrocolloids* **17**, 63–72 (2003).

8. Bragd, P. L., Besemer, a C. & Van Bekkum, H. Bromide-free TEMPO-mediated oxidation of primary alcohol groups in starch and methyl alpha-D-glucopyranoside. *Carbohydrate research* **328**, 355–63 (2000).

9. Smith, A. M. The biosynthesis of starch granules. *Biomacromolecules* **2**, 335–41 (2001).

10. Buléon, a, Colonna, P., Planchot, V. & Ball, S. Starch granules: structure and biosynthesis. *International journal of biological macromolecules* **23**, 85–112 (1998).

11. Wesslén, K. B. & Wesslén, B. Synthesis of amphiphilic amylose and starch derivatives. *Carbohydrate Polymers* **47**, 303–311 (2002).

12. Jane, J. *et al.* Physical and Chemical Studies of Taro Starches and Flours. *Cereal Chemistry* **69**, 528–535 (1992).

13. Lu, T.-J., Lin, J.-H., Chen, J.-C. & Chang, Y.-H. Characteristics of taro (Colocasia esculenta) starches planted in different seasons and their relations to the molecular structure of starch. *Journal of agricultural and food chemistry* **56**, 2208–15 (2008).

14. Jobling, S. Improving starch for food and industrial applications. *Current opinion in plant biology* **7**, 210–8 (2004).

15. Blanche, S. & Sun, X. Physical characterization of starch extrudates as a function of melting transitions and extrusion conditions. *Advances in Polymer Technology* **23**, 277–290 (2004).

16. Jenkins, P. J. & Donald, A. M. Gelatinisation of starch: a combined SAXS/WAXS/DSC and SANS study. *Carbohydrate Research* **308**, 133–147 (1998).

17. Karim, A., Norziah, M. & Seow, C. Methods for the study of starch retrogradation. *Food Chemistry* **71**, 9–36 (2000).

18. Gidley, M. J. & Bulpin, P. V. Aggregation of amylose in aqueous systems: the effect of chain length on phase behavior and aggregation kinetics. *Macromolecules* **22**, 341–346 (1989).

19. Miles, M. J., Morris, V. J., Orford, P. D. & Ring, S. G. The roles of amylose and amylopectin in the gelation and retrogradation of starch. *Carbohydrate Research* **135**, 271–281 (1985).

20. Ring, S., Colonna, P. & I'Anson, K. The gelation and crystallisation of amylopectin. *Carbohydrate …* **162**, 277–293 (1987).

21. Morris, V. Starch gelation and retrogradation. *Trends in Food Science & Technology* **1**, 2–6 (1990).

22. Czuchajowska, Z., Sievert, D. & Pomeranz, Y. Enzyme-resistant starch. IV. Effects of complexing lipids. *Cereal Chem* **68**, 537–542 (1991).

23. Nabeshima, E. . & Grossmann, M. V. . Functional properties of pregelatinized and cross-linked cassava starch obtained by extrusion with sodium trimetaphosphate. *Carbohydrate Polymers* **45**, 347–353 (2001).

24. Lim, S. & Seib, P. Preparation and pasting properties of wheat and corn starch phosphates. *Cereal Chemistry* **70**, 137–144 (1993).

25. Hamdi, G., Ponchel, G. & Duchêne, D. Formulation of epichlorohydrin cross-linked starch microspheres. *Journal of microencapsulation* **18**, 373–83 (2001).

26. Bajpai, a K. & Bhanu, S. Dynamics of controlled release of heparin from swellable crosslinked starch microspheres. *Journal of materials science. Materials in medicine* **18**, 1613–21 (2007).

27. Simkovic, I. Cross-linking of starch with 1, 2, 3, 4-diepoxybutane or 1, 2, 7, 8-diepoxyoctane. *Carbohydrate Polymers* **55**, 299–305 (2004).

28. Uslu, M.-K. & Polat, S. Effects of glyoxal cross-linking on baked starch foam. *Carbohydrate Polymers* **87**, 1994–1999 (2012).

29. Reddy, N. & Yang, Y. Citric acid cross-linking of starch films. *Food Chemistry* **118**, 702–711 (2010).

30. Kim, H.-S., Hwang, D.-K., Kim, B.-Y. & Baik, M.-Y. Cross-linking of corn starch with phosphorus oxychloride under ultra high pressure. *Food Chemistry* **130**, 977–980 (2012).

31. Wester, P. & Heijden, C. Van der Carcinogenicity study with epichlorohydrin (CEP) by gavage in rats. *Toxicology* **36**, 325–339 (1985).

32. Rossi, A. M., Migliore, L., Barale, R. & Loprieno, N. In vivo and in vitro mutagenicity studies of a possible carcinogen, trichloroethylene, and its two stabilizers, epichlorohydrin and 1,2-epoxybutane. *Teratogenesis, Carcinogenesis, and Mutagenesis* **3**, 75–87 (1983).

33. Srám, R. J., Tomatis, L., Clemmesen, J. & Bridges, B. A. An evaluation of the genetic toxicity of epichlorohydrin. A report of an expert group of the International Commission for Protection against Environmental Mutagens and Carcinogens. *Mutation research* **87**, 299–319 (1981).

34. Moad, G. Chemical modification of starch by reactive extrusion. *Progress in Polymer Science* **36**, 218–237 (2011).

35. Xie, F., Yu, L., Liu, H. & Chen, L. Starch Modification Using Reactive Extrusion. *Starch - Stärke* **58**, 131–139 (2006).

36. Lenaerts, V., Dumoulin, Y. & Mateescu, M. Controlled release of theophylline from cross-linked amylose tablets. *Journal of Controlled Release* **15**, 39–46 (1991).

37. Simi, C. K. & Emilia Abraham, T. Hydrophobic grafted and cross-linked starch nanoparticles for drug delivery. *Bioprocess and biosystems engineering* **30**, 173–80 (2007).

38. Shi, A., Li, D., Wang, L., Li, B. & Adhikari, B. Preparation of starch-based nanoparticles through high-pressure homogenization and miniemulsion cross-linking: Influence of various process parameters on particle size and stability. *Carbohydrate Polymers* **83**, 1604–1610 (2011).

39. Santander-Ortega, M. J. *et al.* Nanoparticles made from novel starch derivatives for transdermal drug delivery. *Journal of controlled release : official journal of the Controlled Release Society* **141**, 85–92 (2010).

40. Yu, D., Xiao, S., Tong, C., Chen, L. & Liu, X. Dialdehyde starch nanoparticles: Preparation and application in drug carrier. *Chinese Science Bulletin* **52**, 2913–2918 (2007).

41. Xiao, S. *et al.* Dialdehyde starch nanoparticles as antitumor drug delivery system: An in vitro, in vivo, and immunohistological evaluation. *Chinese Science Bulletin* **57**, 3226–3232 (2012).

42. Vargeese, C. *et al.* Efficient activation of nucleoside phosphoramidites with 4,5-dicyanoimidazole during oligonucleotide synthesis. *Nucleic acids research* **26**, 1046–50 (1998).

43. McBride, L. J. & Caruthers, M. H. An investigation of several deoxynucleoside phosphoramidites useful for synthesizing deoxyoligonucleotides. *Tetrahedron Letters* **24**, 245–248 (1983).

44. WATSON, J. D. & CRICK, F. H. C. Molecular Structure of Nucleic Acids: A Structure for Deoxyribose Nucleic Acid. *Nature* **171**, 737–738 (1953).

45. Yakovchuk, P., Protozanova, E. & Frank-Kamenetskii, M. D. Base-stacking and base-pairing contributions into thermal stability of the DNA double helix. *Nucleic acids research* **34**, 564–74 (2006).

46. Tyagi, S. & Kramer, F. R. Molecular beacons: probes that fluoresce upon hybridization. *Nature biotechnology* **14**, 303–8 (1996).

47. Simonsson, T. G-quadruplex DNA structures--variations on a theme. *Biological chemistry* **382**, 621–8 (2001).

48. Ma, D.-L. *et al.* Structure-Based Approaches Targeting Oncogene Promoter G-Quadruplexes. *Oncogene and Cancer - From Bench to Clinic* (2013).doi:10.5772/3217

49. Huppert, J. L. Four-stranded nucleic acids: structure, function and targeting of G-quadruplexes. *Chemical Society reviews* **37**, 1375–84 (2008).

50. Harrington, C. The Identification and Characterization of a G4-DNA Resolvase Activity. *Journal of Biological Chemistry* **272**, 24631–24636 (1997).

51. Baran, N., Pucshansky, L., Marco, Y., Benjamin, S. & Manor, H. The SV40 large T-antigen helicase can unwind four stranded DNA structures linked by G-quartets. *Nucleic acids research* **25**, 297–303 (1997).

52. Zeugin, J. & Hartley, J. Ethanol precipitation of DNA. *Focus* **7**, 1–2 (1985).

53. Gaillard, C. & Strauss, F. Ethanol precipitation of DNA with linear polyacrylamide as carrier. *Nucleic acids research* **18**, 378 (1990).

54. Tracy, S. Improved rapid methodology for the isolation of nucleic acids from agarose gels. *Preparative biochemistry* **11**, 251–68 (1981).

55. Fregel, R., González, A. & Cabrera, V. M. Improved ethanol precipitation of DNA. *Electrophoresis* **31**, 1350–2 (2010).

56. Bartram, A., Poon, C. & Neufeld, J. Nucleic acid contamination of glycogen used in nucleic acid precipitation and assessment of linear polyacrylamide as an alternative co-precipitant. *BioTechniques* **47**, 1019–22 (2009).

57. Winkler, W. C. & Breaker, R. R. Regulation of bacterial gene expression by riboswitches. *Annual review of microbiology* **59**, 487–517 (2005).

58. Tuerk, C. & Gold, L. Systematic evolution of ligands by exponential enrichment: RNA ligands to bacteriophage T4 DNA polymerase. *Science* **249**, 505–510 (1990).

59. Ellington, A. D. & Szostak, J. W. In vitro selection of RNA molecules that bind specific ligands. *Nature* **346**, 818–22 (1990).

60. Huizenga, D. E. & Szostak, J. W. A DNA aptamer that binds adenosine and ATP. *Biochemistry* **34**, 656–65 (1995).

61. Stojanovic, M. N., De Prada, P. & Landry, D. W. Aptamer-based folding fluorescent sensor for cocaine. *Journal of the American Chemical Society* **123**, 4928–31 (2001).

62. Lee, J.-O. *et al.* Aptamers as molecular recognition elements for electrical nanobiosensors. *Analytical and bioanalytical chemistry* **390**, 1023–32 (2008).

63. Ono, A. & Togashi, H. Highly selective oligonucleotide-based sensor for mercury(II) in aqueous solutions. *Angewandte Chemie (International ed. in English)* **43**, 4300–2 (2004).

64. Schultze, P., Macaya, R. & Feigon, J. Three-dimensional solution structure of the thrombin-binding DNA aptamer d (GGTTGGTGTGGTTGG). *Journal of molecular biology* **235**, 1532–47 (1994).

65. Ng, E. W. M. *et al.* Pegaptanib, a targeted anti-VEGF aptamer for ocular vascular disease. *Nature reviews. Drug discovery* **5**, 123–32 (2006).

66. Sefah, K., Shangguan, D., Xiong, X., O'Donoghue, M. B. & Tan, W. Development of DNA aptamers using Cell-SELEX. *Nature protocols* **5**, 1169–85 (2010).

67. Bates, P. J., Laber, D. a, Miller, D. M., Thomas, S. D. & Trent, J. O. Discovery and development of the G-rich oligonucleotide AS1411 as a novel treatment for cancer. *Experimental and molecular pathology* **86**, 151–64 (2009).

68. Shum, K.-T., Zhou, J. & Rossi, J. J. Nucleic Acid Aptamers as Potential Therapeutic and Diagnostic Agents for Lymphoma. *Journal of Cancer Therapy* **04**, 872–890 (2013).

69. Girvan, A. C. *et al.* AGRO100 inhibits activation of nuclear factor-κB (NF-κB) by forming a complex with NF-κB essential modulator (NEMO) and nucleolin. *Molecular cancer therapeutics* **5**, 1790–9 (2006).

70. Bates, P. J. Antiproliferative Activity of G-rich Oligonucleotides Correlates with Protein Binding. *Journal of Biological Chemistry* **274**, 26369–26377 (1999).

71. Derenzini, M. The AgNORs. *Micron (Oxford, England : 1993)* **31**, 117–20 (2000).

72. Nakanishi, C. & Toi, M. Nuclear factor-κB inhibitors as sensitizers to anticancer drugs. *Nature reviews. Cancer* **5**, 297–309 (2005).

73. Reyes-Reyes, E. M., Teng, Y. & Bates, P. J. A new paradigm for aptamer therapeutic AS1411 action: uptake by macropinocytosis and its stimulation by a nucleolin-dependent mechanism. *Cancer research* **70**, 8617–29 (2010).

74. Soundararajan, S., Chen, W., Spicer, E. K., Courtenay-Luck, N. & Fernandes, D. J. The nucleolin targeting aptamer AS1411 destabilizes Bcl-2 messenger RNA in human breast cancer cells. *Cancer research* **68**, 2358–65 (2008).

75. Guo, J. *et al.* Aptamer-functionalized PEG-PLGA nanoparticles for enhanced anti-glioma drug delivery. *Biomaterials* **32**, 8010–20 (2011).

76. Hernandez, F. J., Hernandez, L. I., Pinto, A., Schäfer, T. & Özalp, V. C. Targeting cancer cells with controlled release nanocapsules based on a single aptamer. *Chemical communications (Cambridge, England)* **49**, 1285–7 (2013).

77. Cao, Z. *et al.* Reversible cell-specific drug delivery with aptamer-functionalized liposomes. *Angewandte Chemie (International ed. in English)* **48**, 6494–8 (2009).

78. Aravind, A. *et al.* AS1411 aptamer tagged PLGA-lecithin-PEG nanoparticles for tumor cell targeting and drug delivery. *Biotechnology and bioengineering* **109**, 2920–31 (2012).

79. Özalp, V. C. & Schäfer, T. Aptamer-based switchable nanovalves for stimuli-responsive drug delivery. *Chemistry (Weinheim an der Bergstrasse, Germany)* **17**, 9893–6 (2011).

80. Nandi, S. & Winter, H. H. Swelling Behavior of Partially Cross-Linked Polymers: A Ternary System. *Macromolecules* **38**, 4447–4455 (2005).

81. Piskur, J. & Rupprecht, a Aggregated DNA in ethanol solution. *FEBS letters* **375**, 174–8 (1995).

82. Nazarenko, I., Pires, R., Lowe, B., Obaidy, M. & Rashtchian, A. Effect of primary and secondary structure of oligodeoxyribonucleotides on the fluorescent properties of conjugated dyes. *Nucleic acids research* **30**, 2089–195 (2002).

83. Torimura, M. *et al.* Fluorescence-quenching phenomenon by photoinduced electron transfer between a fluorescent dye and a nucleotide base. *Analytical sciences : the international journal of the Japan Society for Analytical Chemistry* **17**, 155–60 (2001).

84. Bates, F., French, D. & Rundle, R. Amylose and amylopectin content of starches determined by their iodine complex formation. *Journal of the American Chemical Society* **65**, 142–148 (1943).

85. Rundle, R. E., Foster, J. F. & Baldwin, R. R. On the Nature of the Starch--Iodine Complex. *Journal of the American Chemical Society* **66**, 2116–2120 (1944).

86. Yu, X., Houtman, C. & Atalla, R. H. The complex of amylose and iodine. *Carbohydrate Research* **292**, 129–141 (1996).

87. Saïd Azizi Samir, M. A., Alloin, F., Paillet, M. & Dufresne, A. Tangling Effect in Fibrillated Cellulose Reinforced Nanocomposites. *Macromolecules* **37**, 4313–4316 (2004).

88. Dhar, S., Gu, F. X., Langer, R., Farokhzad, O. C. & Lippard, S. J. Targeted delivery of cisplatin to prostate cancer cells by aptamer functionalized Pt(IV) prodrug-PLGA-PEG nanoparticles. *Proceedings of the National Academy of Sciences of the United States of America* **105**, 17356–61 (2008).

89. Cole, A. J. *et al.* Polyethylene glycol modified, cross-linked starch-coated iron oxide nanoparticles for enhanced magnetic tumor targeting. *Biomaterials* **32**, 2183–93 (2011).

90. Nagayasu, a, Uchiyama, K. & Kiwada, H. The size of liposomes: a factor which affects their targeting efficiency to tumors and therapeutic activity of liposomal antitumor drugs. *Advanced drug delivery reviews* **40**, 75–87 (1999).

91. Choi, H. S. *et al.* Renal clearance of quantum dots. *Nature biotechnology* **25**, 1165–70 (2007).

92. Longmire, M., Choyke, P. L. & Kobayashi, H. Clearance properties of nano-sized particles and molecules as imaging agents: considerations and caveats. *Nanomedicine (London, England)* **3**, 703–17 (2008).

93. Singh, R. & Lillard, J. W. Nanoparticle-based targeted drug delivery. *Experimental and molecular pathology* **86**, 215–23 (2009).

94. Maeda, H., Wu, J., Sawa, T., Matsumura, Y. & Hori, K. Tumor vascular permeability and the EPR effect in macromolecular therapeutics: a review. *Journal of controlled release : official journal of the Controlled Release Society* **65**, 271–84 (2000).

95. Tanaka, T., Shiramoto, S., Miyashita, M., Fujishima, Y. & Kaneo, Y. Tumor targeting based on the effect of enhanced permeability and retention (EPR) and the mechanism of receptor-mediated endocytosis (RME). *International journal of pharmaceutics* **277**, 39–61 (2004).

96. De Nooy, A. E. J., Besemer, A. C. & Van Bekkum, H. Selective oxidation of primary alcohols mediated by nitroxyl radical in aqueous solution. Kinetics and mechanism. *Tetrahedron* **51**, 8023–8032 (1995).

97. Fraschini, C. & Vignon, M. R. Selective oxidation of primary alcohol groups of beta-cyclodextrin mediated by 2,2,6,6-tetramethylpiperidine-1-oxyl radical (TEMPO). *Carbohydrate research* **328**, 585–9 (2000).

98. Kato, Y., Matsuo, R. & Isogai, a Oxidation process of water-soluble starch in TEMPO-mediated system. *Carbohydrate Polymers* **51**, 69–75 (2003).

99. Evier, E. I., Nooy, A. E. J. De, Besemer, A. C. A., Bekkum, H. Van & De Nooy, A. Highly selective nitroxyl radical-mediated oxidation of primary alcohol groups in water-soluble glucans. *Carbohydrate research* **269**, 89–98 (1995).

100. Nakajima, N. & Ikada, Y. Mechanism of amide formation by carbodiimide for bioconjugation in aqueous media. *Bioconjugate chemistry* **6**, 123–30 (1995).

101. Fischer, M. J. E. Amine coupling through EDC/NHS: a practical approach. *Methods in molecular biology (Clifton, N.J.)* **627**, 55–73 (2010).

102. LePecq, J. B. & Paoletti, C. A fluorescent complex between ethidium bromide and nucleic acids. Physical-chemical characterization. *Journal of molecular biology* **27**, 87–106 (1967).

103. Sjöback, R., Nygren, J. & Kubista, M. Absorption and fluorescence properties of fluorescein. *Spectrochimica Acta Part A: Molecular and Biomolecular Spectroscopy* **51**, L7–L21 (1995).

104. Martin, M. M. & Lindqvist, L. The pH Dependence of Fluorescein Fluorescence. *Journal of Luminescence* **10**, 381–390 (1975).

105. Zhu, H. *et al.* Fluorescent Intensity of Dye Solutions under Different pH Conditions. *Journal of ASTM International* **2**, 12926 (2005).

106. Masters, J. R. HeLa cells 50 years on: the good, the bad and the ugly. *Nature reviews. Cancer* **2**, 315–9 (2002).

107. Capes-Davis, A. *et al.* Check your cultures! A list of cross-contaminated or misidentified cell lines. *International journal of cancer. Journal international du cancer* **127**, 1–8 (2010).

108. Hovanessian, A. G. *et al.* Surface expressed nucleolin is constantly induced in tumor cells to mediate calcium-dependent ligand internalization. *PloS one* **5**, e15787 (2010).